

On exact truncation of backward waves in elastrodynamics

Wangtao Lu¹

January 16, 2023

Abstract

For elastic wave scattering problems in unbounded anisotropic media, the existence of backward waves makes classic truncation techniques fail completely. This paper is concerned with an exact truncation technique for terminating backward elastic waves. We derive a closed form of elastrodynamic Green's tensor based on the method of Fourier transform and design two fundamental principles to ensure its physical correctness. We present a rigorous theory to completely classify the propagation behavior of Green's tensor, thus proving a conjecture posed by Bécache, Fauqueux and Joly (**J. Comp. Phys.**, **188**, **2003**) regarding a necessary and sufficient condition of the non-existence of backward waves. Using Green's tensor, we propose a new radiation condition to characterize anisotropic scattered waves at infinity. This leads to an exact transparent boundary condition (TBC) to truncate the unbounded domain, regardless the existence of backward waves or not. We develop a fast algorithm to evaluate Green's tensor and a high-accuracy scheme to discretize the TBC. A number of experiments are carried out to validate the correctness and efficiency of the new TBC.

1 Introduction

Acoustic, electromagnetic (optical), and elastic (seismic) waves form the fundamental class of waves in real world, and have presented tremendous applications in the past centuries, ranging from wireless communication, medical imaging, to underwater and geological explorations, etc. Mathematically, the propagation behavior of such three waves scattered by bounded obstacles are governed by three well-known partial differential equations named after Helmholtz, Maxwell and Navier, respectively. Specifically, if the propagation medium is isotropic and homogeneous, all of the three scattering problems can be formulated in close relation with Helmholtz's exterior problem,

$$-\Delta u(x) - k^2 u(x) = 0, \quad \mathbb{R}^d \setminus \overline{D}, \quad (1) \quad \{\text{eq:helm}\}$$

¹Corresponding author. School of Mathematical Sciences, Zhejiang University, Hangzhou 310027, China. Email: wangtaolu@zju.edu.cn. This author is partially supported by NSFC Grant 12174310 and by NSF of Zhejiang Province for Distinguished Young Scholars (LR21A010001).

$$u = f, \quad \text{on } \partial D, \quad (2) \quad \{\text{eq:helm:bc}\}$$

where $d = 2, 3$ indicates the dimension of the problem, $x = (x_1, \dots, x_d)$, $\Delta = \sum_{j=1}^d \partial_j^2$ is the d -dimensional Laplacian with $\partial_j = \frac{\partial}{\partial x_j}$, u is a time-harmonic wave field, $k > 0$ is a constant depending on the medium property, D represents a bounded domain, and f represents a given function.

This classic problem, firstly studied by Helmholtz in 1860, encountered an essential difficulty: the solution may be non-unique. This wasn't resolved until, in 1912, Sommerfeld in his pioneer work [35] firstly proved the uniqueness by imposing an extra but necessary condition for u at infinity:

$$\lim_{r \rightarrow \infty} r^{(d-1)/2} \left(\frac{\partial u}{\partial r} - \mathbf{i} k u \right) = 0, \quad r = |x|, \quad \mathbf{i} = \sqrt{-1}, \quad (3) \quad \{\text{eq:src}\}$$

uniformly w.r.t. all directions x/r . This condition, now known as the famous Sommerfeld radiation condition (SRC), reveals an important fact:

“Any scattered wave must behave as an outgoing wave $r^{-(d-1)/2} e^{\mathbf{i} k r}$ at infinity”.

It had subsequently been extended to the Silver-Müller-Sommerfeld radiation condition [34, 28] for Maxwell's equations and the Kupradze-Sommerfeld radiation condition [20] for Navier's equations. For related well-posedness theories, we refer readers to [14, 26, 20] and the references therein for details. Because of the significance of the underlying motivation of SRC (3), we briefly review its derivation first, according to the fabulous review paper [33]. Throughout the rest of the paper, we assume $d = 2$ for simplicity.

1.1 Motivation of SRC

To derive (3), we require Green's function of (1),

$$\Phi_k(x; y) := \frac{\mathbf{i}}{4} H_0^{(1)}(k|x - y|) = \frac{\mathbf{i}}{4\pi} \int_{-\infty}^{\infty} \frac{e^{\mathbf{i}\sqrt{k^2 - \xi^2}|x_2 - y_2| + \mathbf{i}\xi(x_1 - y_1)}}{\sqrt{k^2 - \xi^2}} d\xi, \quad (4) \quad \{\text{eq:phik}\}$$

a.k.a. a fundamental solution, solving

$$-\Delta \Phi_k(x; y) - k^2 \Phi_k(x; y) = \delta(x - y), \quad (5) \quad \{\text{eq:gov:Phi}\}$$

where $y = (y_1, y_2)$ denotes the source point and $H_m^{(1)}$ denotes the first-kind Hankel function of m -th order.

Let $B(0, r)$ be a disk of sufficiently large radius r and $\Omega = B(0, r) \setminus \overline{D}$. Apply Green's third identity in Ω ,

$$u(x) = \left[\int_{\partial B(0, r)} + \int_{\partial D} \right] [\partial_{\nu(y)} \Phi_k(y; x) u(y) - \Phi_k(y; x) \partial_{\nu} u(y)] ds(y), \quad x \in \Omega, \quad (6)$$

where ν is the outer unit normal of $\partial\Omega$. Sommerfeld's original idea is to propose certain condition to ensure the first integral over $\partial B(0, r)$ vanishes as $r \rightarrow \infty$, i.e.,

$$\lim_{r \rightarrow \infty} \int_{\partial B(0, r)} [\partial_{\nu(y)} \Phi_k(y; x) u(y) - \Phi_k(y; x) \partial_{\nu} u(y)] ds(y) = 0, \quad (7) \quad \{\text{eq:surc}\}$$

uniformly for x in any bounded domain, since it directly yields Green's exterior representation formula

$$u(x) = \int_{\partial D} [\partial_{\nu(y)} \Phi_k(y; x) u(y) - \Phi_k(y; x) \partial_{\nu} u(y)] ds(y), x \in \mathbb{R}^2 \setminus \overline{D}. \quad (8) \quad \{\text{eq:grep:helm}\}$$

By

$$\partial_{|y|}^j \Phi_k(x; y) = (\mathbf{i}k)^j \sqrt{\frac{2}{\pi k|y|}} e^{\mathbf{i}k|y|} + \mathcal{O}(|y|^{-3/2}), j = 0, 1, 2, \quad |y| \rightarrow \infty,$$

uniformly for x in any bounded domain, (7) becomes

$$\lim_{r \rightarrow \infty} e^{\mathbf{i}kr} \int_0^{2\pi} \sqrt{r} [\mathbf{i}ku - \partial_r u] d\theta = 0, \quad (9)$$

which immediately motivates SRC (3). Roughly speaking, SRC (3) is an elegant way of stating the equivalent but unpleasant condition (7), which will be referred to as Sommerfeld's unpleasant radiation condition (SURC).

1.2 Truncation techniques based on SRC

With SRC condition (3), the well-posedness of Helmholtz's exterior problem (1) had been settled [14]. However, it remains challenging to numerically compute u due to the unbounded computational domain. Nevertheless, SRC motivates three widely used truncation techniques.

Due to the special form of Laplacian in polar coordinates (or spherical coordinates if $d = 3$), the method of variable separation is applicable in $r \geq r_0$, for some sufficiently large $r_0 > 0$ so that $D \subset B(0, r_0)$, to express

$$u(r, \theta) = \sum_{n=0}^{\infty} [a_n H_n^{(1)}(kr) + b_n H_n^{(2)}(kr)] e^{\mathbf{i}m\theta}, \quad r \geq r_0.$$

SRC implies that $b_n = 0$ for $n \in \mathbb{N}$ since $H_n^{(2)}$ is not outgoing and does not satisfy (3). Then, the above induces a variable-separation based transparent boundary condition (TBC)

$$\partial_r u = \Lambda u, \quad \text{on } r = r_0, \quad (10) \quad \{\text{eq:tbc1:helm}\}$$

for a bounded operator $\Lambda : H^{1/2}(\partial B(0, r_0)) \rightarrow H^{-1/2}(\partial B(0, r_0))$. The second, more general approach is based on Green's representation formula (8). Letting x approaching ∂D and using standard jump relations yield a boundary-integral-equation (BIE) based TBC

$$\mathcal{A}u + \mathcal{B}\partial_{\nu} u = 0, \quad \text{on } \partial D, \quad (11) \quad \{\text{eq:tbc2:helm}\}$$

for two bounded integral operators $\mathcal{A} : H^{1/2}(\partial D) \rightarrow H^{1/2}(\partial D)$ and $\mathcal{B} : H^{-1/2}(\partial D) \rightarrow H^{1/2}(\partial D)$. For related works using analogous TBC techniques, readers are referred to [2, 14, 17, 27, 19, 4] and the references therein.

The previous two approaches induce nonlocal boundary conditions to truncate the unbounded domain. The third, more attractive approach is to develop a local

boundary condition by introducing an artificial absorbing medium, the so-called perfectly matched layer (PML), originally developed by Berenger [7] in 1994 for time-domain Maxwell's equations. Mathematically, PML introduces the following complexified coordinates [13]

$$\tilde{x}_i = x_i + \mathbf{i} \int_0^{x_i} \sigma_i(t) dt, i = 1, 2, \quad (12) \quad \{\text{eq:pml:xi}\}$$

where $\sigma_i(t) = 0$ for $|t| \leq L_i$, and are nonzero for $L_i \leq |t| \leq L_i + d_i$. The regions of nonzero σ_i constitute the PML region. Any scattered wave u satisfying SRC (3) and hence (8) shall be complexified to

$$u(\tilde{x}) = \int_{\partial D} [\partial_{\nu(y)} \Phi_k(y; \tilde{x}) u(y) - \Phi_k(y; \tilde{x}) \partial_\nu u(y)] ds(y), \quad x \in \mathbb{R}^2 \setminus \overline{D}.$$

As has been indicated in [9], the outgoing behavior of Φ_k making its complexification $\Phi_k(y; \tilde{x})$ decays exponentially in the PML and so does $u(\tilde{x})$. Therefore, it is spectrally accurate to impose a zero Dirichlet boundary condition on the PML boundary, i.e.,

$$u(\tilde{x}) = 0, \quad \text{on} \quad \{x : |x_1| = L_1 + d_1 \text{ or } |x_2| = L_2 + d_2\}. \quad (13) \quad \{\text{eq:pmlbc}\}$$

Numerically computing $u(\tilde{x})$ recovers $u(x)$ with high accuracy outside the PML for $\tilde{x} = x$. Due to its simplicity and nearly zero reflection for outgoing waves, PML has, since its development, been widely used in the simulation of a variety of wave propagation problems [36, 30]. Readers are referred to [9, 10, 11, 12, 21, 24] for the spectral convergence theories of the PML truncation for various scattering problems, and to [15] for an approximate but effective absorbing boundary condition due to Engquist and Majda. Besides, the author and his collaborators have recently developed a hybrid truncation technique that combines PML and a BIE-based TBC technique for scattering problems in complicated structures [25, 23, 16, 38].

1.3 Elastrodynamics: failure of SRC

As has been seen, the related truncation techniques rely mostly on the outgoing behavior of the scattered field due to the isotropicity of the media. Unfortunately, such a significant prerequisite breaks down in anisotropic media, due to the possible existence of backward waves. Physically speaking, a backward wave refers to a wave with an always outgoing group velocity, the physically correct direction of energy transport [18], propagates incoming from the infinity. For Helmholtz's scattering problem (1), there is no backward wave since a plane wave $e^{\mathbf{i}(v_1 x_1 + v_2 x_2)}$ of directional vector $v = (v_1, v_2)$ satisfies $k = \sqrt{v_1^2 + v_2^2}$ so that the group velocity $\nabla_v k$ always coincides with the propagation direction v . This is unfortunately not true in elastrodynamics with anisotropic media commonly encountered in practice [8]. Consequently, it becomes a fundamental task to precisely characterize and accurately simulate the propagation behavior of elastic waves in such media. This is the main objective of the current paper.

Let us start with a Dirichlet-type exterior problem. Now, D denotes a bounded rigid body with its complement $\mathbb{R}^2 \setminus \overline{D}$ filled by a homogeneous but anisotropic

elastic medium. A time-harmonic scattered wave $u = [u_1, u_2]^T$ due to an incident wave $u^{\text{inc}} = [u_1^{\text{inc}}, u_2^{\text{inc}}]^T$ imping upon D is then governed by Navier's equation

$$-\nabla \cdot \sigma(u) - \rho\omega^2 u = 0, \quad \mathbb{R}^2 \setminus \overline{D}, \quad (14) \quad \{\text{eq:gov:2d}\}$$

$$u(x) = -u^{\text{inc}}, \quad \text{on } \partial D, \quad (15) \quad \{\text{eq:dir:bc}\}$$

where (15) is due to the zero total wave $u^{\text{tot}} = u + u^{\text{inc}}$ on ∂D , $\nabla = [\partial_1, \partial_2]^T$, ω is the frequency of the incident wave, σ is the stress tensor satisfying

$$\sigma = C\epsilon(u), \quad (16)$$

$C = [C_{ijkl}]_{i,j,k,l=1}^2$ is a fourth-order tensor, the strain tensor $\epsilon(u) = [\epsilon_{ij}(u)]$ with

$$\epsilon_{ij}(u) = \frac{1}{2}(\partial_i u_j + \partial_j u_i),$$

and

$$\nabla \cdot \sigma = \begin{bmatrix} \partial_1 \sigma_{11} + \partial_2 \sigma_{12} \\ \partial_1 \sigma_{12} + \partial_2 \sigma_{22} \end{bmatrix}. \quad (17)$$

Using the Voigt notation [8], C can be represented by a 3×3 positive symmetric matrix denoted by

$$C = \begin{bmatrix} c_{11} & c_{12} & c_{13} \\ c_{12} & c_{22} & c_{23} \\ c_{13} & c_{23} & c_{33} \end{bmatrix},$$

and (14) becomes

$$-\partial_1(A_{11}\partial_1 u + A_{12}\partial_2 u) - \partial_2(A_{21}\partial_1 u + A_{22}\partial_2 u) - \rho\omega^2 u = 0, \quad \text{in } \mathbb{R}^2 \setminus \overline{D}, \quad (18) \quad \{\text{eq:gov}\}$$

where

$$A_{11} = \begin{bmatrix} c_{11} & c_{13} \\ c_{13} & c_{33} \end{bmatrix}, \quad A_{12} = A_{21}^T = \begin{bmatrix} c_{13} & c_{12} \\ c_{33} & c_{23} \end{bmatrix}, \quad A_{22} = \begin{bmatrix} c_{33} & c_{23} \\ c_{23} & c_{22} \end{bmatrix}.$$

To illustrate the basic idea, we consider orthotropic media which assume $c_{13} = c_{23} = 0$ throughout this paper; the case when $c_{13} \neq 0$ or $c_{23} \neq 0$ can be analyzed with no technical difficulty. Thus, the nonzero elements c_{ij} must satisfy

$$(C_0) \begin{cases} (i) & c_{11}, c_{22}, c_{33} > 0, c_{11}c_{22} - c_{12}^2 > 0; \\ (ii) & c_{12} + c_{33} \neq 0, \end{cases}$$

where $(C_0)(ii)$ is to avoid the decoupling of u_1 and u_2 .

Similar to Helmholtz's problem (1), Navier's problem (18) necessarily requires an accurate radiation condition at infinity, which remains absent so far to the author's best knowledge. Even worse, the failure of SRC makes the extension of the aforementioned truncation techniques precarious. Specifically, the first technique via a variable-separation based TBC like (10) fails as variable separations may not work in the first place, let alone the invalidity of SRC. The second technique based on a BIE-based TBC like (11) now faces a new challenging: Green's tensor. A closed-form of Green's tensor based on d -dimensional Fourier transform is trivial

[22]. However, it remains unclear whether it reveals the true radiation behavior of the scattered field, as Green's tensor needs not to be unique.

The third technique based on PML now becomes more subtle. Bécache *et al.* in [5] rigorously justified the instability of PML in elastodynamics due to the existence of backward waves, which blow up in the PML. They further derived a sufficient condition to ensure the stability of PML, and conjectured its necessity, the proof of which is incomplete yet. To try to resolve the instability, Appelö and Kreiss [3] and Savadatti and Guddati [31, 32] subsequently designed new types of PMLs, which applied only for a limited class of elastic media. Recently, Bécache *et al.* [5] developed a half-space matching method to solve Navier's problem (18). They applied the simple one-dimensional Fourier transform along four straight lines surrounding the obstacle D , proposed rules to capture backward waves, and successfully developed a truncation technique by solving four half-space problems.

1.4 Methodology: opportunity of SURC

The methodology of the current work closely follows Sommerfeld's philosophy for Helmholtz's problem (1). We believe that SURC (7) can be generalized to prescribe the asymptotic behavior of acoustic, electromagnetic, and elastic scattered waves in homogeneous but whatever anisotropic media, if the associated Green tensor/function is correctly selected! Meanwhile, the selecting principle should obey the same rule in choosing Φ_k for Helmholtz's problem (1), as discussed below.

The integral form of $\Phi_k(x; y)$ in (4), a.k.a. Sommerfeld's integral, is derived by Fourier transforming (5) w.r.t. the single variable x_1 (generally, the $d - 1$ variables x_1, \dots, x_{d-1}), matching the Fourier transform of Φ_k for the other variable x_2 at $x_2 = y_2$, and an inverse Fourier transform finally. Then, the radiation behavior of Φ_k is completely determined by a proper choice of branch cut of $\sqrt{k^2 - \xi^2}$; choosing a wrong branch cut could lead to incoming Green's function $\overline{\Phi}_k(x; y)$. This is completely resolved by replacing the real path with Sommerfeld's integral path (SIP), a complex path going from an infinity in Quadrant II to the origin, and then to another infinity in Quadrant IV. Now $\sqrt{k^2 - \xi^2}$ is always complex (except at $\xi = 0$) and the basic rule is simply letting $\text{Im}(\sqrt{k^2 - \xi^2}) \geq 0$ to ensure the boundedness of the integrand in (4). Moreover, by replacing k with $k + \mathbf{i}\delta$ for $\delta > 0$, it is well known that $\Phi_{k+\mathbf{i}\delta}$ decays exponentially and that

$$\Phi_k(x; y) = \lim_{\delta \rightarrow 0^+} \Phi_{k+\mathbf{i}\delta}(x; y),$$

indicating that Φ_k is the limit of dissipative Green's function $\Phi_{k+\mathbf{i}\delta}$ and hence is physically correct. The above constitutes the basic idea of selecting physically correct Green's tensor for Navier's problem (18). Upon an analog of SURC (7) and a carefully selected Green tensor, an analog of Green's exterior representation formula (8) for Navier's problem can be derived. Then, the second TBC truncation technique becomes straightforwardly extendable, as it does not care at all about the outgoing or incoming behavior of u !

The rest of this paper is organized as follows. In section 2, we derive Green's tensor for Navier's problem (18). In section 3, we present a rigorous theory to

completely classify the propagation behavior of Green's tensor for any tensor C satisfying (C_0) , thus providing an affirmative answer to the aforementioned conjecture in [6]. In section 4, a fast algorithm is proposed to evaluate Green's tensor and its derivatives. In section 5, we propose an analog of SURC (7) for Navier's problem (18), leading to a new TBC analogous to (11), and carry out a number of numerical experiments to justify the correctness of the TBC. In section 6, we study two typical scattering problems and demonstrate the efficiency of the new TBC by a number of examples. In section 7, we conclude this paper by raising some significant problems.

2 Elastodynamic Green's tensor

The two-dimensional elastodynamic Green tensor

$$G(x; y) = \begin{bmatrix} G_{11}(x; y) & G_{12}(x; y) \\ G_{21}(x; y) & G_{22}(x; y) \end{bmatrix}$$

excited by a source point $y \in \mathbb{R}^2$, is defined as a solution of

$$- [\partial_1(A_{11}\partial_1 + A_{12}\partial_2) + \partial_2(A_{21}\partial_1 + A_{22}\partial_2) + \rho\omega^2] G(x; y) = I\delta(x - y), \quad (19) \quad \{\text{eq:gov:G}\}$$

where I denotes the 2×2 identity matrix. This problem has infinitely many solutions. In this section, we propose two fundamental principles to single out a unique and physically reasonable solution $G(x; y)$, and derive its closed form for any tensor C satisfying (C_0) by the method of Fourier transform.

For simplicity, we assume $y = 0$ for the moment, and write $G(x)$ short for $G(x; 0)$. Consider $G_1 = [G_{11}, G_{21}]^T$ first. For a generic function $f(x)$, let

$$\hat{f}(x_2; \xi) = \int_{-\infty}^{\infty} f(x) e^{i\xi x_1} dx_1$$

be the x_1 -Fourier transform of f . Then, x_1 -Fourier transforming the first column of (19) yields

$$i\xi(c_{12} + c_{33}) \frac{d}{dx_2} \hat{G}_{21} + c_{33} \frac{d^2}{dx_2^2} \hat{G}_{11} + (\rho\omega^2 - c_{11}\xi^2) \hat{G}_{11} = -\delta(x_2), \quad (20) \quad \{\text{eq:gov:1:fre}\}$$

$$i\xi(c_{12} + c_{33}) \frac{d}{dx_2} \hat{G}_{11} + c_{22} \frac{d^2}{dx_2^2} \hat{G}_{21} + (\rho\omega^2 - c_{33}\xi^2) \hat{G}_{21} = 0. \quad (21) \quad \{\text{eq:gov:2:fre}\}$$

This implies the following continuity conditions

$$[\hat{G}_{11}]_{x_2=0} = 0, \quad [\hat{G}'_{11}]_{x_2=0} = -c_{33}^{-1}, \quad (22) \quad \{\text{eq:cond:1}\}$$

$$[\hat{G}_{21}]_{x_2=0} = 0, \quad [\hat{G}'_{21}]_{x_2=0} = 0, \quad (23) \quad \{\text{eq:cond:2}\}$$

where $[\cdot]_{x_2=0}$ indicates the jump of the quantity from $x_2 = 0+$ to $x_2 = 0-$.

For $x_2 \neq 0$, we obtain

$$\left[c_{33} \frac{d^2}{dx_2^2} + (\rho\omega^2 - c_{11}\xi^2) \right] \hat{G}_{11} = -i\xi(c_{12} + c_{33}) \frac{d}{dx_2} \hat{G}_{21}, \quad (24) \quad \{\text{eq:gov:12}\}$$

$$\left[c_{22} \frac{d^2}{dx_2^2} + (\rho\omega^2 - c_{33}\xi^2) \right] \hat{G}_{21} = -\mathbf{i}\xi(c_{12} + c_{33}) \frac{d}{dx_2} \hat{u}_{11}. \quad (25) \quad \{\text{eq:gov:21}\}$$

Thus, \hat{G}_{j1} is governed by the following characteristic equation

$$c_{33}c_{22}\hat{G}_{j1}^{(4)} + [\rho\omega^2\beta_0 + \xi^2\beta_1] \hat{G}_{j1}^{(2)} + (\rho\omega^2 - c_{11}\xi^2)(\rho\omega^2 - c_{33}\xi^2)\hat{G}_{j1} = 0, \quad (26) \quad \{\text{eq:cha}\}$$

for $j = 1, 2$, where

$$\beta_0 = c_{22} + c_{33}, \quad (27) \quad \{\text{eq:b0}\}$$

$$\beta_1 = c_{12}^2 + 2c_{12}c_{33} - c_{11}c_{22}. \quad (28) \quad \{\text{eq:b1}\}$$

A simple derivation shows that

$$\hat{G}_{j1}(x_2; \xi) = \begin{cases} p_j^+(\xi)e^{\mathbf{i}\mu_+(\xi^2)x_2} + q_j^+(\xi)e^{\mathbf{i}\mu_-(\xi^2)x_2}, & x_2 > 0; \\ p_j^-(\xi)e^{-\mathbf{i}\mu_+(\xi^2)x_2} + q_j^-(\xi)e^{-\mathbf{i}\mu_-(\xi^2)x_2}, & x_2 < 0, \end{cases}$$

for $j = 1, 2$, where p_j^\pm and q_j^\pm are unknowns to be determined and μ_\pm^2 are roots of

$$c_{33}c_{22}\zeta^2 - [\rho\omega^2\beta_0 + \xi^2\beta_1]\zeta + (\rho\omega^2 - c_{11}\xi^2)(\rho\omega^2 - c_{33}\xi^2) = 0. \quad (29) \quad \{\text{eq:cha:mu}\}$$

Here, we keep only two propagation waves in each region to ensure the boundedness of \hat{G} at $\xi = \pm\infty$. Thus,

$$\mu_\pm^2(\xi^2) = \frac{[\rho\omega^2\beta_0 + \xi^2\beta_1] \pm \sqrt{\Delta(\xi^2)}}{2c_{33}c_{22}}, \quad (30) \quad \{\text{eq:mupm}\}$$

$$\Delta(\xi^2) = \rho^2\omega^4\alpha_0 + 2\rho\omega^2\xi^2\alpha_1 + \xi^4\alpha_2, \quad (31) \quad \{\text{eq:Delta}\}$$

where $\alpha_0 = (c_{22} - c_{33})^2$ and

$$\alpha_1 = (c_{22} + c_{33})(c_{12} + c_{33})^2 - (c_{22} - c_{33})(c_{11}c_{22} - c_{33}^2), \quad (32)$$

$$\alpha_2 = (c_{11}c_{22} - c_{12}^2)(c_{11}c_{22} - (c_{12} + 2c_{33})^2). \quad (33) \quad \{\text{eq:alpha2}\}$$

In the above, three special square-root functions $\sqrt{\Delta}$ and $\sqrt{\mu_\pm^2}$ appear. To correctly capture the propagation behavior of G , we propose two fundamental principles to select proper branch cuts for them. As c_{11}^{-1} and c_{33}^{-1} are zeros of μ_\pm^2 and hence branch points of μ_\pm , indicating that $\mu_\pm(\xi^2)$ may not be analytic for $\xi \in \mathbb{R}$. To resolve this, we make use of the aforementioned SIP. Let

$$\chi(t) = \begin{cases} t, & 0 \leq t \leq 1; \\ 1, & \text{otherwise.} \end{cases} \quad (34)$$

The following path

$$\{z(\xi; \epsilon_0) = \text{sgn}(\xi)\sqrt{\xi^2 - \epsilon\mathbf{i}} : \epsilon(\xi^2) = \epsilon_0^2\chi(\xi^2/\epsilon_0), \xi \in \mathbb{R}, 0 < \epsilon_0 \ll 1\} \quad (35) \quad \{\text{eq:z:sip}\}$$

in the complex plane is a typical SIP and shall be used throughout this paper unless otherwise indicated (c.f. Remark 5), where sgn is the standard sign function and, for simplicity, the arguments of z and ϵ shall be suppressed frequently. Unless otherwise indicated, the branch cut of a usual square-root function shall be chosen as the negative real axis so that its argument is limited to $(-\frac{\pi}{2}, \frac{\pi}{2}]$. Thus, SIP goes from $-\infty + 0\mathbf{i}$ to the origin in Quadrant II, and then to $+\infty - 0\mathbf{i}$ in Quadrant IV; here $\pm 0\mathbf{i}$ indicates the path approaches the real axis at infinity from above and below, respectively. The first principle is

(P1) μ_{\pm} must be analytic along SIP for $0 < \epsilon_0 \ll 1$;

this is based on that G is analytic for $x_2 \neq 0$. Based on (P1), we define

$$\mu_{\pm}(\xi^2) = \lim_{\epsilon_0 \rightarrow 0^+} \mu_{\pm}(z^2(\xi; \epsilon_0)). \quad (36) \quad \{\text{eq:}\mu:\text{def}\}$$

The second principle is

$$(P2) \quad \text{Im}(\mu_{\pm}(\xi^2)) \geq 0, \quad \forall \xi \in \mathbb{R};$$

otherwise, \hat{G}_{1j} blows up at $x_2 = \pm\infty$. In section 3, we shall determine the branch cuts of the three functions to realize (P1) and (P2). We first make some preliminary remarks regarding the choice of branch cuts for the three functions.

Remark 1. *The branch cut of $\sqrt{\Delta}$ is not so essential as it just affects the definitions of μ_{\pm}^2 in (30); we only require that $\sqrt{\Delta}$ is analytic along the SIP to protect (P1). To achieve (P2), we may directly adopt the positive real axis as the branch cuts of $\sqrt{\mu_{\pm}^2}$ so that $\arg \mu_{\pm} \in [0, \pi)$. However, this cannot guarantee (P1).*

From the continuity conditions (22) and (23) and the two governing equations (24) and (25), the eight unknowns p_j^{\pm} and q_j^{\pm} can be derived on the SIP to bypass zeros of Δ and μ_{\pm}^2 . They are given by

$$p_2^+ = -p_2^- = -q_2^+ = q_2^- = \frac{-\mathbf{i}z(c_{12} + c_{33})c_{33}^{-1}}{2c_{22}(\mu_+^2 - \mu_-^2)} = \frac{-\mathbf{i}z(c_{12} + c_{33})}{2\sqrt{\Delta(z^2)}}, \quad (37) \quad \{\text{eq:p2}\}$$

and

$$p_1^+ = p_1^- = -\mathbf{i} \frac{[-c_{22}\mu_+^2(z^2) + (\rho\omega^2 - c_{33}z^2)]}{2\sqrt{\Delta(z^2)}\mu_+(z^2)}, \quad (38) \quad \{\text{eq:p1}\}$$

$$q_1^+ = q_1^- = \mathbf{i} \frac{[-c_{22}\mu_-^2(z^2) + (\rho\omega^2 - c_{33}z^2)]}{2\sqrt{\Delta(z^2)}\mu_-(z^2)}. \quad (39) \quad \{\text{eq:q1}\}$$

Then, G_1 can be obtained via the following inverse Fourier transform,

$$G_1(x) = \frac{1}{2\pi} \int_{\mathbb{R}} \hat{G}_1(x; \xi) e^{-\mathbf{i}\xi x_1} d\xi = \frac{1}{2\pi} \int_{\text{SIP}} \hat{G}_1(x; z) e^{-\mathbf{i}z x_1} dz,$$

where the second equality holds by Cauchy's theorem and by the two principles (P1) and (P2). Consequently, by a simple translation, one obtains $G_1(x; y) = [G_{11}(x; y); G_{21}(x; y)]^T$ given by

$$G_{11}(x; y) = \frac{1}{2\pi} \int_{\mathbb{R}} \left[p_1^{x_1}(\xi) e^{\mathbf{i}\mu_+(\xi^2)|x_2-y_2|} + q_1^{x_1}(\xi) e^{\mathbf{i}\mu_-(\xi^2)|x_2-y_2|} \right] e^{\mathbf{i}\xi|x_1-y_1|} d\xi, \quad (40) \quad \{\text{eq:green11}\}$$

$$G_{21}(x; y) = \frac{-\text{sgn}[(x_1 - y_1)(x_2 - y_2)]}{2\pi} \int_{\mathbb{R}} p_2^{x_1}(\xi) \left[e^{\mathbf{i}\mu_+(\xi^2)|x_2-y_2|} - e^{\mathbf{i}\mu_-(\xi^2)|x_2-y_2|} \right] e^{\mathbf{i}\xi|x_1-y_1|} d\xi, \quad (41) \quad \{\text{eq:green21}\}$$

where $p_1^{x_1} = p_1^+$, $p_2^{x_1} = p_2^+$, and $q_1^{x_1} = q_1^+$. Similarly, the second column of $G(x; y)$, $G_2(x; y) = [G_{12}(x; y); G_{22}(x; y)]^T$ is derived to be

$$G_{12}(x; y) = -\frac{\text{sgn}[(x_1 - y_1)(x_2 - y_2)]}{2\pi} \int_{\mathbb{R}} p_1^{x_2}(\xi) \left[e^{i\mu_+(\xi^2)|x_2-y_2|} - e^{i\mu_-(\xi^2)|x_2-y_2|} \right] e^{i\xi|x_1-y_1|} d\xi, \quad (42) \quad \{\text{eq:green12}\}$$

$$G_{22}(x; y) = \frac{1}{2\pi} \int_{\mathbb{R}} \left[p_2^{x_2}(\xi) e^{i\mu_+(\xi^2)|x_2-y_2|} + q_2^{x_2}(\xi) e^{i\mu_-(\xi^2)|x_2-y_2|} \right] e^{i\xi|x_1-y_1|} d\xi, \quad (43) \quad \{\text{eq:green22}\}$$

where $p_1^{x_2} = p_2^{x_1}$, and

$$p_2^{x_2} = -i \frac{-c_{33}\mu_+^2 + (\rho\omega^2 - c_{11}\xi^2)}{2\sqrt{\Delta(\xi^2)}\mu_+(\xi^2)}, \quad (44)$$

$$q_2^{x_2} = i \frac{-c_{33}\mu_-^2 + (\rho\omega^2 - c_{11}\xi^2)}{2\sqrt{\Delta(\xi^2)}\mu_-(\xi^2)}. \quad (45)$$

Clearly, Green's tensor G is symmetric, satisfies $G(x; y) = G(x - y)$, and obeys the usual reciprocal relation

$$G(x; y) = G(y; x).$$

To simplify the presentation, we shall assume $\rho\omega^2 = 1$ unless otherwise indicated. For numerical purposes, we split G into two parts as

$$G(x) = G^+(x) + G^-(x), \quad (46) \quad \{\text{eq:G:sp}\}$$

with

$$G^+(x) = [G_{ij}^+] = \frac{1}{2\pi} \int_{\mathbb{R}} \begin{bmatrix} p_1^{x_1}(\xi) & -\text{sgn}(x_1 x_2) p_2^{x_1}(\xi) \\ -\text{sgn}(x_1 x_2) p_2^{x_1}(\xi) & p_2^{x_2}(\xi) \end{bmatrix} e^{i\mu_+|x_2| + i\xi|x_1|} d\xi,$$

$$G^-(x) = [G_{ij}^-] = \frac{1}{2\pi} \int_{\mathbb{R}} \begin{bmatrix} q_1^{x_1}(\xi) & \text{sgn}(x_1 x_2) p_2^{x_1}(\xi) \\ \text{sgn}(x_1 x_2) p_1^{x_2}(\xi) & q_2^{x_2}(\xi) \end{bmatrix} e^{i\mu_-|x_2| + i\xi|x_1|} d\xi.$$

From the above, it can be seen that $G(x)$ consists of plane waves

$$P_{\pm}(x; \xi) := e^{i\mu_{\pm}|x_2| + i\xi x_1}, \xi \in \mathbb{R}.$$

Clearly, (P2) ensures $\text{Im}(\mu_{\pm}) \geq 0$ so that $P_{\pm}(x; \xi)$ is bounded and will never blow up at $x = \infty$ for all $\xi \in \mathbb{R}$. However, (P2) cannot determine the sign of $\text{Re}(\mu_{\pm})$, which determines the propagation behavior of $P_{\pm}(x; \xi)$. Basically, there are two possible situations:

$$P_{\pm}(x; \xi) \text{ is } \begin{cases} \text{outgoing along } x_2\text{-direction if } \text{Re}(\mu_{\pm}) \geq 0; \\ \text{incoming along } x_2\text{-direction if } \text{Re}(\mu_{\pm}) \leq 0. \end{cases}$$

The outgoing/incoming waves $P_{\pm}(x; \xi)$ are referred to as the so-called forward/backward propagating waves. Note that the ambiguity for $\text{Re}(\mu_{\pm}) = 0$ is safe here since it corresponds to the case when $P_{\pm}(x; \xi)$ propagates purely along x_1 -direction, and, if $\text{Im}(\mu_{\pm}) > 0$, decays along x_2 -direction. In section 3, we shall present a complete classification of Green's tensor G for any tensor C satisfying (C_0) in the sense that

the branch cuts of $\sqrt{\Delta}$ and $\sqrt{\mu_{\pm}^2}$ as well as the propagation behavior of $P(x; \xi)$ are completely revealed. Before that, we present a lemma that reveals the locations where $\mu_{\pm}^2(z^2)$ cross the real axis as z travels along the SIP. They play a central role in identifying the branch cuts of $\sqrt{\mu_{\pm}^2}$.

Lemma 1. *For $0 < \epsilon_0 \ll 1$, the two paths $\{\mu_{\pm}^2(z^2) : \xi \in \mathbb{R}\}$ in \mathbb{C} together cross the real axis at most twice (Here and hereafter, we only count the number of nonzero values of ξ^2). Specifically,*

(i). *If $\beta_1 = 0$, two crossing points occur at the same point*

$$\xi_0^2 = \frac{c_{11} + c_{33}}{2c_{11}c_{33}} > 0, \quad (47) \quad \{\text{eq:xi20}\}$$

with $\mu_+^2(\xi_0^2 - \mathbf{i}\epsilon)\mu_-^2(\xi_0^2 - \mathbf{i}\epsilon) < 0$;

(ii). *If $\beta_1 \neq 0$, the crossing points, if any, are*

$$\zeta_0 = \frac{2c_{11}c_{33}\xi^2 - (c_{11} + c_{33})}{\beta_1}, \quad (48) \quad \{\text{eq:rootformu}\}$$

with $\xi^2 > 0$ solving

$$\alpha_2\xi^4 + 2\alpha_1\xi^2 - \frac{\gamma_2}{c_{11}c_{33}} + \beta_1^2\epsilon^2 = 0, \quad (49) \quad \{\text{eq:realroot}\}$$

where

$$\gamma_2 = \{(c_{12} + c_{33})^2 - c_{11}(c_{22} - c_{33})\} \times \{(c_{12} + c_{33})^2 + c_{33}(c_{22} - c_{33})\}. \quad (50) \quad \{\text{eq:g2}\}$$

Proof. With $z^2 = \xi^2 - \epsilon\mathbf{i}$ in place of ξ^2 in (29), the crossing points correspond to real roots of the following equation

$$\zeta^2 - \frac{\beta_0 + (\xi^2 - \epsilon\mathbf{i})\beta_1}{c_{33}c_{22}}\zeta + \frac{(1 - c_{11}(\xi^2 - \epsilon\mathbf{i}))(1 - c_{33}(\xi^2 - \epsilon\mathbf{i}))}{c_{33}c_{22}} = 0.$$

Suppose it has a real root ζ_0 . Equating the imaginary and real parts of the two sides yields

$$\frac{\beta_1\epsilon}{c_{33}c_{22}}\zeta_0 + \frac{(c_{11} + c_{33})\epsilon - 2c_{11}c_{33}\epsilon\xi^2}{c_{33}c_{22}} = 0,$$

and

$$\zeta_0^2 - \frac{\beta_0 + \beta_1\xi^2}{c_{33}c_{22}}\zeta_0 + \frac{(1 - c_{11}\xi^2)(1 - c_{33}\xi^2) - c_{11}c_{33}\epsilon^2}{c_{33}c_{22}} = 0.$$

If $\beta_1 = 0$, $\xi^2 = \xi_0^2$ so that $(1 - c_{11}\xi_0^2)(1 - c_{33}\xi_0^2) < 0$ and $\mu_+^2(\xi_0^2 - \mathbf{i}\epsilon)\mu_-^2(\xi_0^2 - \mathbf{i}\epsilon) < 0$. Suppose now $\beta_1 \neq 0$. For $\xi^2 > 0$ so that $\epsilon > 0$, (48) holds and hence $\xi^2 > 0$ must be a root of (49). \square

3 Classification of Green's tensor

In this section, we determine the branch cuts of $\sqrt{\Delta}$ and $\sqrt{\mu_{\pm}^2}$, and, as a by-product, give a complete classification of G at infinity. We discuss G at $x_2 = \pm\infty$ only; for G at $x_1 = \pm\infty$, one simply permutes c_{11} and c_{22} in C to swap x_1 and x_2 . It turns out that the sign of $\min_{\xi \in \mathbb{R}} \Delta(\xi^2)$ significantly affects the behavior of G at infinity. Thus, we distinguish two cases: $\min_{\xi \in \mathbb{R}} \Delta(\xi^2) \geq 0$ and $\min_{\xi \in \mathbb{R}} \Delta(\xi^2) < 0$.

3.1 Purely outgoing Green's tensor for $\min_{\xi \in \mathbb{R}} \Delta(\xi^2) \geq 0$

To ensure $\min \Delta(\xi^2) \geq 0$, Bécache, Fauqueux and Joly [6] have found the following sufficient and necessary condition: the tensor C must satisfy

$$(BFJ)_{x_2}^0 : \begin{cases} (C_1)' \quad \gamma_1 := \{(c_{12} + c_{33})^2 - c_{22}(c_{11} - c_{33})\} \times \{(c_{12} + c_{33})^2 + c_{33}(c_{11} - c_{33})\} \leq 0, \\ (C_2) \begin{cases} (i) \quad (c_{12} + 2c_{33})^2 \leq c_{11}c_{22} \\ (ii) \quad (c_{12} + c_{33})^2 < c_{11}c_{22} + c_{33}^2 \end{cases}, \\ \text{one of } \begin{cases} (C_3)_1 \quad (c_{12} + c_{33})^2 \leq (c_{11} - c_{33})(c_{22} - c_{33}), \\ (C_3)_2 \quad (c_{22} + c_{33})(c_{12} + c_{33})^2 \geq (c_{22} - c_{33})(c_{11}c_{22} - c_{33}^2). \end{cases} \end{cases}$$

Remark 2. As indicated in [6], $(C_1)'$ and $(C_2)(ii)$ are superfluous based on the observation that

$$\begin{aligned} \beta_1 &= c_{12}(c_{12} + 2c_{33}) - c_{11}c_{22} \leq (|c_{12}| - \sqrt{c_{11}c_{22}})\sqrt{c_{11}c_{22}} < 0, \\ 0 &\leq \Delta(-\beta_0\beta_1^{-1}) = -4\gamma_1c_{22}c_{33}\beta_1^{-2}. \end{aligned}$$

Nevertheless, we keep them here for completeness.

We first figure out the branch cut of $\sqrt{\Delta(z^2)}$ for $z \in \text{SIP}$ with $\epsilon_0 \ll 1$ under $(BFJ)_{x_2}^0$. By

$$\Delta(z^2) = \Delta(\xi^2) - \alpha_2\epsilon^2 - 2(\alpha_2\xi^2 + \alpha_1)\epsilon i. \quad (51)$$

and by $\min \Delta(\xi^2) \geq 0$, it is straightforward to see that $\Delta(z^2)$ never crosses the negative axis. Thus, the negative real axis can serve as the branch cut of $\sqrt{\Delta}$ when $\min \Delta(\xi^2) > 0$. Note that if $\min \Delta(\xi^2) = 0$, $\sqrt{\Delta}$ becomes entire.

3.1.1 A strong condition

We start from a strong condition that guarantees no backward waves. It states as follows:

(OC) $_{x_2}$ For $0 < \epsilon_0 \ll 1$, $P_{\pm}(x; z)$ is purely outgoing for any $z \in \text{SIP}$.

Permuting c_{11} and c_{22} in $(C_1)'$ to get

$$(C_1) \quad \gamma_2 \leq 0,$$

we obtain

$$(BFJ)_{x_2} \quad (C_1) \ \& \ (C_2) \ \& \ [(C_3)_1 \mid (C_3)_2],$$

where $\&$ and \mid denote the logical “and” and “or” operators, respectively.

Remark 3. Condition $(BFJ)_{x_2}$ is stronger than $(BFJ)_{x_2}^0$. See Medium (II) in section 3.3 with $\gamma_2 > 0$ but $\min \Delta(\xi^2) \geq 0$. Moreover, it is straightforward to deduce $\gamma_2 < 0$ if $\alpha_1 \leq 0$.

We prove that $(BFJ)_{x_2}$ is a sufficient and necessary condition of (OC) $_{x_2}$ in the following. First, we identify the branch cuts of $\sqrt{\mu_{\pm}^2}$.

Lemma 2. For any $0 < \epsilon_0 \ll 1$,

$$\operatorname{Im}(\mu_{\pm}^2(z^2(\xi^2; \epsilon_0))) \geq 0, \quad \forall \xi \in \mathbb{R},$$

holds if and only if condition (BFJ) $_{x_2}$ holds. The equality holds iff $\xi = 0$.

Proof. “If”. Case $\xi = 0$ is trivial. Suppose $\xi > 0$ in the following. (BFJ) $_{x_2}$ implies

$$\gamma_2 \leq 0 \ \& \ \alpha_2 \geq 0 \ \& \ \beta_1 < 0 \ \& \ [\alpha_1 \geq 0 \mid \alpha_1^2 - \alpha_0 \alpha_2 \leq 0].$$

We claim that (49) cannot hold. This is clear for $\alpha_1 \geq 0$. Suppose $\alpha_1 < 0$ and $\alpha_1^2 \leq \alpha_0 \alpha_2$ now. Thus $\alpha_2 > 0$ and

$$\begin{aligned} & \alpha_1^2 - \alpha_2 \left[\frac{-\gamma_2}{c_{11}c_{33}} + \beta_1^2 \epsilon^2 \right] \\ &= c_{11}^{-1} c_{33}^{-1} (c_{12} + c_{33})^2 \beta_1^2 [(c_{12} + c_{33})^2 - (c_{11} - c_{33})(c_{22} - c_{33})] - \alpha_2 \beta_1^2 \epsilon^2 < 0, \end{aligned}$$

and again (49) cannot hold. Consequently, $\mu_{\pm}^2(z^2)$ never touch the real axis unless $\xi = 0$. At $\xi^2 = +\infty$, it is not hard to see that

$$\operatorname{Im}(\mu_{\pm}^2(z^2)) \approx \frac{-\beta_1 \mp \sqrt{\alpha_2}}{2c_{33}c_{22}} \epsilon > 0,$$

so that the proof can be concluded by noticing that $\mu_{\pm}^2(z^2)$ is continuous for $z \in \text{SIP}$. “Only if”. We claim that $\Delta(\xi^2)$ should be nonnegative for all $\xi \in \mathbb{R}$ first. Suppose, otherwise, for some $\xi_0 \in \mathbb{R}$, $\Delta(\xi_0^2) < 0$. Thus, one of $\pm \sqrt{\Delta(\xi_0^2)}$ must have strictly negative imaginary part so that for $\epsilon \ll 1$, $\min(\operatorname{Im}(\mu_{\pm}^2(\xi_0^2 - \mathbf{i}\epsilon))) < 0$, a contradiction. Consequently, $\alpha_2 \geq 0$ so that (C_2) holds, and one of $(C_3)_1$ and $(C_3)_2$ must hold by (C_0) .

We only need to verify (C_1) . We prove it by contradiction. Suppose (C_1) does not hold, i.e., $\gamma_2 > 0$. Then, $\beta_1^2 \alpha_0 - \alpha_1^2 = -4c_{22}c_{33}\gamma_2 < 0$, so that

$$\beta_1 \sqrt{\alpha_0} + |\alpha_1| > 0,$$

as $\beta_1 < 0$. Thus,

$$\alpha_2 \alpha_0 - \alpha_1^2 \leq \beta_1^2 \alpha_0 - \alpha_1^2 < 0,$$

so that $(C_3)_1$ does not hold. Then, $(C_3)_2$ must hold so that $\alpha_1 > 0$. If $\alpha_0 > 0$, then $\Delta(\xi^2) \geq \Delta(0) > 0$ so that

$$\operatorname{Im}(\sqrt{\Delta(\xi^2 - \mathbf{i}\epsilon)}) = -\frac{\alpha_2 \xi^2 + \alpha_1}{\sqrt{\Delta(\xi^2)}} \epsilon + \mathcal{O}(\epsilon^2).$$

Consider

$$F(\xi^2) := \beta_1^2 \Delta(\xi^2) - (\alpha_2 \xi^2 + \alpha_1)^2 = (\beta_1^2 - \alpha_2) \alpha_2 \xi^4 + 2(\beta_1^2 - \alpha_2) \alpha_1 \xi^2 + (\beta_1^2 \alpha_0 - \alpha_1^2).$$

The minimum of $F(\xi^2)$ is negative since $\beta_1^2 \alpha_0 < \alpha_1^2$. There exists $\xi_* \in \mathbb{R} \setminus \{0\}$ such that

$$|\beta_1| < \frac{|\alpha_2 \xi_*^2 + \alpha_1|}{\sqrt{\Delta(\xi_*^2)}}.$$

It is straightforward to verify that for $\epsilon \ll 1$,

$$\operatorname{Im}(\mu_+^2(\xi_*^2 - \mathbf{i}\epsilon)) \leq \frac{1}{2} \left[|\beta_1| - \frac{|\alpha_2 \xi_*^2 + \alpha_1|}{\sqrt{\Delta(\xi_*^2)}} \right] \epsilon < 0,$$

a contradiction. Thus, we must have $\alpha_0 = 0$ so that $\xi = 0$ becomes a branch point of $\sqrt{\Delta(\xi^2 - \mathbf{i}\epsilon)}$. Nevertheless, for $0 < \xi^2 \leq \epsilon_0$, $\epsilon = \xi^2 \epsilon_0$ so that

$$\sqrt{\Delta(\xi^2 - \mathbf{i}\epsilon)} = |\xi| \sqrt{2\alpha_1(1 - \epsilon_0 \mathbf{i}) + \alpha_2(1 - \epsilon_0 \mathbf{i})^2 \xi^2} = |\xi| \sqrt{2\alpha_1} \sqrt{1 - \epsilon_0 \mathbf{i}} + \mathcal{O}(|\xi|^3).$$

The proof is concluded by observing

$$\operatorname{Im}(\mu_+^2(\xi^2 - \mathbf{i}\epsilon)) = -\frac{|\xi| \sqrt{2\alpha_1} \epsilon_0}{2} + \mathcal{O}(\epsilon_0^{3/2}) < 0.$$

□

Lemma 2 suggests to use the positive real axis as the branch cut of $\sqrt{\mu_\pm^2}$ so that $\mu_\pm(z^2) \in \mathbb{C}^{++}$ for all $z \in \text{SIP}$. Consequently, we obtain the equivalence of $(\text{BFJ})_{x_2}$ and $(\text{OC})_{x_2}$.

{thm:x2}

Theorem 1. For $0 < \epsilon_0 \ll 1$, $(\text{BFJ})_{x_2} \iff (\text{OC})_{x_2}$.

3.1.2 A weak condition

Condition $(\text{OC})_{x_2}$ requires $\mu_\pm(z^2) \in \overline{\mathbb{C}^{++}}$ for all $z \in \text{SIP}$ for $0 < \epsilon_0 \ll 1$, which implies $\mu_\pm(\xi^2) \in \overline{\mathbb{C}^{++}}$ for all $\xi \in \mathbb{R}$ by the definition (36), but not vice versa. Taking $\epsilon_0 = 0$ to replace SIP in $(\text{OC})_{x_2}$ by the real axis, we obtain a weaker condition

$$(\text{OC})_{x_2}^0: \quad (\text{OC})_{x_2} \text{ with } \epsilon_0 = 0.$$

To justify the equivalence of $(\text{OC})_{x_2}^0$ and $(\text{BFJ})_{x_2}^0$, we need a more delicate lemma than Lemma 2.

{lem:wkx2}

Lemma 3. For all $\xi \in \mathbb{R}$,

$$\arg(\mu_-^2(z^2(\xi^2; \epsilon_0))) \in [0, \pi), \quad (52) \quad \{\text{eq:weakres1}\}$$

$$\arg(\mu_+^2(z^2(\xi^2; \epsilon_0))) \in (-\delta_0 \epsilon_0, \pi + \delta_0 \epsilon_0), \quad (53) \quad \{\text{eq:weakres2}\}$$

for $0 < \epsilon_0 \ll 1$, if and only if condition $(\text{BFJ})_{x_2}^0$ holds. Here $\delta_0 > 0$ is a constant independent of ϵ_0 .

Proof. “If”. As in the proof of Lemma 2, $(C_3)_1$ implies (C_1) so that (52) and (53) follow immediately. We now assume $(C_3)_2$ holds but $(C_3)_1$ and (C_1) not. Thus, $\gamma_2 > 0$, $\alpha_2 \geq 0$, $\alpha_1 \geq 0$, and $\beta_1 < 0$. By (51) and by $\min_{\xi \in \mathbb{R}} \Delta(\xi^2) > 0$, $\operatorname{Im}(\sqrt{\Delta(z^2)}) \leq 0$ so that

$$\operatorname{Im}(\mu_-^2(z^2)) \geq \frac{-\beta_1 \epsilon}{2c_{33}c_{22}} > 0,$$

for all $0 \neq z \in \text{SIP}$. In other words, $\mu_-^2(z^2)$ never touches the real axis and $\arg \mu_-^2(z^2) \in (0, \pi)$. We now consider $\arg \mu_+^2(z^2)$. Observe that (49) has only one positive root

$$\xi_*^2(\epsilon) = \frac{-\alpha_1 + \sqrt{\alpha_1^2 + \frac{\alpha_2 \gamma_2}{c_{11} c_{33}}}}{\alpha_2} + \mathcal{O}(\epsilon^2),$$

where the prefactor in \mathcal{O} -term is independent of ϵ^2 and the first term on the right-hand side takes a limit when $\alpha_2 = 0$. Thus, $\mu_+^2(\xi^2)$ must cross the positive real axis once only at ξ_*^2 .

As in the proof of Lemma 2, $\text{Im}(\mu_+^2) > 0$ at $\xi^2 = \infty$. Thus, we can find a constant $\delta_1 > 0$, such that $\text{Im}(\mu_+^2(z^2)) > 0$ for $\xi^2 - \xi_*^2(0) \geq \delta_1$. For $\xi^2 \in [0, \xi_*^2(0) + \delta_1]$, it can be easily seen that $|\text{Im}(\mu_+^2(z^2))| \leq \delta_2 \epsilon$ for some constant δ_2 independent of ϵ_0 . If $|\text{Re}(\mu_+^2(z^2))|$ is uniformly bounded below from some constant greater than 0 w.r.t. ϵ_0 , then the proof is concluded. This indicates that we only need to consider the case when ξ^2 is near c_{11}^{-1} or c_{33}^{-1} , where $\mu_+^2(\xi^2)$ is zero.

Since $\mu_-^2(\xi^2)$ is strictly decreasing, it has exactly one root considering $\mu_-^2(0)\mu_-^2(+\infty) < 0$ and hence $\mu_+^2(\xi^2)$ also has exactly one root. We thus distinguish two cases:

(i) $\mu_-^2(c_{11}^{-1}) = 0$ such that $\mu_+^2(c_{33}^{-1}) = 0$. Thus, $\mu_+^2(c_{11}^{-1}) > 0$ and $\mu_-^2(c_{33}^{-1}) < 0$ considering $\Delta(c_{jj}^{-1}) > 0$ for $j = 1, 3$. But μ_-^2 is decreasing so that $c_{11} > c_{33}$. Now suppose $\xi^2 = c_{33}^{-1} + \delta$ for $|\delta| \leq \delta_3$, a sufficiently small constant independent of ϵ_0 . Then,

$$\mu_+^2(z^2) = \frac{c_{11}c_{33}\delta^2 + (c_{11} - c_{33})\delta - c_{11}c_{33}\epsilon^2 + [(c_{33} - c_{11}) - 2c_{11}c_{33}\delta]\epsilon \mathbf{i}}{c_{33}c_{22}\mu_-^2(z^2)}.$$

Here, the numerator is strictly below the real axis and $\arg \mu_-^2(z^2) \in (\pi - \delta_4 \epsilon, \pi)$ for some constant δ_4 independent of ϵ_0 . Thus, $\arg \mu_+^2(z^2) \in (0, \pi + \delta_4 \epsilon)$.

(ii) $\mu_-^2(c_{33}^{-1}) = 0$ such that $\mu_+^2(c_{11}^{-1}) = 0$. One can just permute c_{11} and c_{33} in the arguments above to obtain the same conclusion.

(53) follows by combining the above results.

“Only if”. Firstly, $\Delta(\xi^2) \geq 0$ for all $\xi \in \mathbb{R}$, since, otherwise, one of $\mu_{\pm}^2(\xi_0^2)$ must lie strictly below the real axis for some $\xi_0 \in \mathbb{R}$ and (53) fails at $z^2 = \xi_0^2 - \mathbf{i}\epsilon$. Thus, $(C_2)(i)$ and one of $(C_3)_1$ and $(C_3)_2$ must hold, implying $(\text{BFJ})_{x_2}^0$ by Remark 2. \square

The above lemma indicates that we can choose the positive real axis as the branch cut of $\sqrt{\mu_-^2}$ and a ray $[0, \infty)e^{-i\theta_0}$ in Quadrant IV as the branch cut of $\sqrt{\mu_+^2}$, where $\theta_0 > 0$ is a sufficiently small constant independent of ϵ_0 . Letting $\epsilon_0 \rightarrow 0^+$, we obtain the following theorem immediately.

Theorem 2. $(\text{OC})_{x_2}^0 \iff (\text{BFJ})_{x_2}^0$.

{thm:x2w}

Remark 4. In [6], the authors proved that $(\text{BFJ})_{x_2}^0$ is sufficient to stabilize a PML along the x_2 -direction. They further conjectured that $(\text{BFJ})_{x_2}^0$ should be necessary, the proof of which is yet incomplete. Theorem 2 shows that $(\text{BFJ})_{x_2}^0$ is a sufficient and necessary condition for $P_{\pm}(x; \xi)$ to be purely outgoing. It is clear that such a property holds for any $\rho > 0$ and $\omega \in \mathbb{R}$. By the inverse Fourier transform w.r.t. ω , the associated time-domain Green tensor consists of purely outgoing waves as well. According to section 1.2, this is an equivalent condition for a PML to stably absorbing such time-domain Green’s tensor and any hence the solution of any associated Cauchy problem in the x_2 -direction. Consequently, this affirmatively resolves the conjecture.

3.2 Partially incoming Green's tensor for $\min_{\xi \in \mathbb{R}} \Delta(\xi^2) < 0$

By Theorem 2, $(OC)_{x_2}^0$ does not hold only if $(BFJ)_{x_2}^0$ is violated, and hence $\min_{\xi \in \mathbb{R}} \Delta(\xi^2) < 0$. We now justify that the previously proposed two principles (P1) and (P2) are still applicable for any general tensor C satisfying (C_0) but not $(BFJ)_{x_2}^0$. As in the proof of Lemma 3, $(C_3)_1$ must not hold, i.e., $\alpha_1^2 - \alpha_0\alpha_2 > 0$. Then, breaking $(BFJ)_{x_2}^0$ indicates that the following three inequalities

$$\beta_1 < 0, \quad \alpha_2 \geq 0, \quad \text{and} \quad \alpha_1 \geq 0,$$

cannot hold simultaneously. Two possible situations arise: $\min_{\xi \in \mathbb{R}} \Delta(\xi^2) \in (-\infty, 0)$ and $\min_{\xi \in \mathbb{R}} \Delta(\xi^2) = -\infty$. The related results are presented in the following two theorems.

{thm:4.2.1}

Theorem 3. Suppose $\min_{\xi \in \mathbb{R}} \Delta(\xi^2) \in (-\infty, 0)$ and $0 < \epsilon_0 \ll 1$. The positive real axis simultaneously serves as the branch cuts of $\sqrt{\Delta}$ and $\sqrt{\mu_{\pm}^2}$, fulfilling the two principles (P1) and (P2). The plane wave $P_+(x; \xi)$ is purely outgoing for all $\xi \in \mathbb{R}$, while the plane wave $P_-(x; \xi)$ is outgoing for all $\xi^2 \in \mathbb{R}/(\xi_1^2(0), \xi_2^2(0))$, but incoming for $\xi^2 \in (\xi_1^2(0), \xi_2^2(0))$, where $\xi_1^2(0)$ and $\xi_2^2(0)$ are the two positive roots of (49) for $\epsilon_0 = 0$.

Proof. Since $\min_{\xi \in \mathbb{R}} \Delta(\xi^2) \in (-\infty, 0)$, $\alpha_2 > 0$, $\alpha_1 < 0$, $\beta_1 < 0$ and $\gamma_2 < 0$ (c.f. Remark 3). By (51), $\Delta(z^2)$ for $z \in \text{SIP}$ never crosses the positive real axis, which shall serve as the branch cut of $\sqrt{\Delta}$. Thus, for $\xi \neq 0$, $\text{Im}(\sqrt{\Delta(z^2)}) > 0$ so that $\text{Im}(\mu_+^2(z^2)) > 0$ and $\mu_+^2(z^2)$ lie completely above the real axis. We can simply choose the positive real axis as the branch cut of $\sqrt{\mu_+^2}$.

As for $\sqrt{\mu_-^2}$, (49) indicates that $\mu_-^2(z^2)$ cross the real axis twice at $\xi_j^2(\epsilon)$, $j = 1, 2$ with $\xi_2^2 > -\frac{\alpha_1}{\alpha_2} > \xi_1^2$ for $0 \neq z \in \text{SIP}$. Recall ξ_0^2 defined in (47). Eq. (49) implies

$$\Delta(\xi_0^2) - \Delta(\xi_j^2) = \frac{(c_{11} - c_{33})^2 \beta_1^2}{4c_{11}^2 c_{33}^2} + \beta_1^2 \epsilon^2 > 0, \quad j = 1, 2, \quad (54) \quad \{\text{eq:xi0:xij}\}$$

so that we must have $\xi_2^2 > \xi_1^2 > \xi_0^2$ or $\xi_0^2 > \xi_2^2 > \xi_1^2$. We claim that $\xi_0^2 < \xi_1^2$. Suppose, otherwise, $\xi_0^2 > \xi_2^2$. Then, $\xi_0^2 > -\frac{\alpha_1}{\alpha_2}$ implies

$$0 < \alpha_2 \xi_0^2 + \alpha_1 = \beta_1(\beta_0 + \beta_1 \xi_0^2).$$

Thus, $\beta_0 + \beta_1 \xi_0^2 < 0$. This together with $\alpha_1 < 0$ and $\alpha_1^2 > \alpha_0 \alpha_2$ implies

$$(c_{11} - c_{33})(c_{22} - c_{33}) < (c_{12} + c_{33})^2 < \max_{j=1,2} \left\{ \frac{c_{jj} - c_{33}}{c_{jj} + c_{33}} (c_{11}c_{22} - c_{33}^2) \right\}.$$

One may check that the above inequality is impossible for any C satisfying (C_0) .

For $\xi_0^2 < \xi_1^2$, (48) implies that $\mu_-^2(z^2)$ crosses the negative real axis twice at ξ_j^2 , $j = 1, 2$ for $0 \neq z \in \text{SIP}$. In other words, μ_-^2 never crosses the positive real axis, which can serve as the branch cut of $\sqrt{\mu_-^2}$. As $\text{Im}(\mu_-^2(z^2)) \geq 0$ for $\xi^2 \ll 1$ or $\xi^2 \gg 1$, μ_-^2 lies below the real axis only for $\xi^2 \in (\xi_1^2(\epsilon), \xi_2^2(\epsilon))$. The proof is concluded by letting $\epsilon_0 \rightarrow 0^+$. \square

{thm:4.2.2}

Theorem 4. Suppose $\min_{\xi \in \mathbb{R}} \Delta(\xi^2) = -\infty$ and $0 < \epsilon_0 \ll 1$. The negative real axis and the positive real axis serve as the branch cuts of $\sqrt{\Delta(z^2)}$ and $\sqrt{\mu_-^2(z^2)}$, respectively, for $z \in \text{SIP}$. The branch cut of $\sqrt{\mu_+^2(z^2)}$ should be chosen as ray $[0, +\infty)e^{-i\theta_0}$ in Quadrant IV if $\gamma_2 > 0$ or the positive real axis if $\gamma_2 \leq 0$. They fulfill the two principles (P1) and (P2). The plane wave $P_+(x; \xi)$ is purely outgoing for all $\xi \in \mathbb{R}$, while the plane wave $P_-(x; \xi)$ is outgoing for $\xi^2 \in [0, \xi_*^2(0)]$ but incoming for $\xi^2 \in (\xi_*^2(0), \infty)$, where $\xi_*^2(0)$ is the single positive root of (49) for $\epsilon_0 = 0$.

Proof. Since $\min_{\xi \in \mathbb{R}} \Delta(\xi^2) = -\infty$, $\alpha_2 \leq 0$. We claim that $\Delta(z^2)$ never crosses the negative real axis as z travels along an SIP for $\epsilon_0 \ll 1$. Otherwise, by (51), $\xi^2 = -\frac{\alpha_1}{\alpha_2}$ and $\Delta(\xi^2) = \max_{\eta \in \mathbb{R}} \Delta(\eta^2) \leq 0$. Thus, $\alpha_0 = 0$ so that $\alpha_1 > 0$. But now $\Delta(\eta^2) > 0$ for $\eta^2 \ll 1$, a contradiction. Consequently, the negative real axis can serve as the branch cut of $\sqrt{\Delta(z^2)}$ for $z \in \text{SIP}$. As for the branch cuts of $\sqrt{\mu_{\pm}^2}$, we distinguish two cases: (i) $\gamma_2 > 0$; (ii) $\gamma_2 \leq 0$.

(i). $\gamma_2 > 0$ so that $\alpha_1 > 0$, $\alpha_2 < 0$, and

$$\beta_1^2 \alpha_0 - \alpha_1^2 = -4c_{22}c_{33}\gamma_2 < 0.$$

Moreover, (49) must have two positive roots denoted by $\xi_1^2(\epsilon)$ and $\xi_2^2(\epsilon)$. This indicates that $\mu_{\pm}^2(z^2)$ together cross the real axis twice at $\xi^2 = \xi_j^2, j = 1, 2$ with $0 < \xi_1^2 < -\frac{\alpha_1}{\alpha_2} < \xi_2^2$. Thus, we must have $\beta_1\sqrt{\alpha_0} - \alpha_1 < 0$ and $\beta_1\sqrt{\alpha_0} + \alpha_1 > 0$. For $\xi^2 \ll 1$, $\epsilon = \epsilon_0|\xi|^2$. If $\alpha_0 > 0$,

$$2c_{22}c_{33}\mu_{\pm}(z^2) \approx \beta_0 - \beta_1\mathbf{i}\epsilon \pm \sqrt{\alpha_0 - 2\alpha_1\mathbf{i}} \approx \beta_0 \pm \sqrt{\alpha_0} - (\beta_1 \pm \frac{\alpha_1}{\sqrt{\alpha_0}})\mathbf{i}\epsilon. \quad (55) \quad \{\text{eq:closeto0:}\}$$

If $\alpha_0 = 0$,

$$2c_{22}c_{33}\mu_{\pm}(z^2) \approx \beta_0 - \beta_1\mathbf{i}\epsilon \pm |\xi|\sqrt{2\alpha_1}\sqrt{1 - \epsilon_0}\mathbf{i} \approx \beta_0 \mp \frac{|\xi|\sqrt{2\alpha_1}}{2}\epsilon_0\mathbf{i}. \quad (56) \quad \{\text{eq:closeto0:}\}$$

At $\xi^2 = +\infty$,

$$2c_{22}c_{33}\mu_{\pm}(z^2) \approx \beta_1\xi^2 \pm \sqrt{|\alpha_2|}\xi^2\mathbf{i}. \quad (57) \quad \{\text{eq:infy}\}$$

Therefore, either of μ_+^2 and μ_-^2 crosses the real axis exactly once. Suppose $\beta_1 \neq 0$ for the moment. By

$$2c_{33}c_{22}\text{Im}(\mu_{\pm}^2(-\alpha_1/\alpha_2 - \mathbf{i}\epsilon)) = -\beta_1\epsilon,$$

it must hold that $\mu_+^2(\xi_2^2 - \mathbf{i}\epsilon)$ and $\mu_-^2(\xi_1^2 - \mathbf{i}\epsilon) \in \mathbb{R}$ if $\beta_1 > 0$, or that $\mu_+^2(\xi_1^2 - \mathbf{i}\epsilon)$ and $\mu_-^2(\xi_2^2 - \mathbf{i}\epsilon) \in \mathbb{R}$ if $\beta_1 < 0$. On the other hand, (54) and

$$\Delta(\xi_1^2) = \Delta(\xi_2^2) = \frac{\gamma_2}{c_{11}c_{33}} - \beta_1^2\epsilon^2 + \alpha_0 > 0,$$

imply that $\xi_1^2 < \xi_0^2 < \xi_2^2$. Consequently, (48) implies $\mu_-^2(z^2)$ crosses the negative real axis once while $\mu_+^2(z^2)$ crosses the positive real axis once. We can use the positive real axis as the branch cut of $\sqrt{\mu_-^2}$. As for $\sqrt{\mu_+^2}$, it holds that $2c_{33}c_{22}\text{Re}(\mu_+^2) \geq \beta_0$ and $|\text{Im}(\mu_+^2)| \leq \delta_2\epsilon$ for $\xi^2 \in [0, \xi_2^2 + \delta_1]$, where constants δ_1 and δ_2 are independent

$\min_{\xi \in \mathbb{R}} \Delta(\xi^2)$	$(-\infty, 0)$	$[0, +\infty)$ (Outgoing)	$\{-\infty\}$
B.C. $\sqrt{\Delta(z^2)}$	$[0, +\infty)$	$(-\infty, 0)$ /entire	
B.C. $\sqrt{\mu_-^2(z^2)}$	$[0, +\infty)$		
B.C. $\sqrt{\mu_+^2(z^2)}$	$[0, +\infty)$	$\gamma_2 \leq 0$: $[0, +\infty)$	
		$\gamma_2 > 0$: $[0, +\infty)e^{-i\theta_0}$	

Table 1: Branch cuts of the three square-root functions $\sqrt{\Delta(z^2)}$, $\sqrt{\mu_-^2(z^2)}$ and $\sqrt{\mu_+^2(z^2)}$ for $z \in \text{SIP}$. Here, B.C. stands for branch cut and $\theta_0 > 0$ is a sufficiently small constant independent of ϵ_0 ; $P_\pm(x; \xi)$ is outgoing along x_2 -direction only when $\min_{\xi \in \mathbb{R}} \Delta(\xi^2) \in [0, +\infty)$; $\sqrt{\Delta(z^2)}$ can be entire if $\min_{\xi \in \mathbb{R}} \Delta(\xi^2) = 0$. {tab:bc}

of ϵ_0 . Thus, we can use ray $[0, \infty)e^{-i\theta_0}$ in Quadrant IV as the branch cut of $\sqrt{\mu_+^2}$. If $\beta_1 = 0$, since $\text{Re}(\sqrt{\Delta}) \geq 0$ for all $z \in \text{SIP}$, $\mu_+^2(\xi_0^2 - i\epsilon) > 0$ so that $\mu_-^2(\xi_0^2 - i\epsilon) < 0$ by Lemma 1. The rest is similar as before.

(ii). $\gamma_2 \leq 0$ so that $\beta_1 < 0$. Suppose first $\alpha_2 < 0$. Then, $\mu_\pm^2(z^2)$ together cross the real axis once at ξ_2^2 with $\xi_2^2 > \max(0, -\frac{\alpha_1}{\alpha_2})$ for $0 \neq z \in \text{SIP}$ by (49). But, (54) implies $\xi_0^2 < \xi_2^2$ so that the crossing point must occur on the negative real axis so that none of $\mu_\pm^2(z^2)$ cross the positive real axis for $0 \neq z \in \text{SIP}$. Thus, the positive real axis can serve as the branch cuts of $\sqrt{\mu_\pm^2}$. If $\alpha_2 = 0$ so that $\alpha_1 < 0$ and $\alpha_0 > 0$. Again, (49) has only one positive root ξ_2^2 with $\xi_2^2 > \xi_0^2$. The rest is similar as before.

To sum up, the above theory indicates that $\mu_-^2(z^2)$ lies below the real axis only when $\xi^2 > \xi_*^2(\epsilon)$, where

$$\xi_*^2(\epsilon) = \begin{cases} \xi_1^2(\epsilon) & \beta_1 > 0, \gamma_2 > 0; \\ \xi_2^2(\epsilon) & \beta_1 < 0; \\ \xi_0^2(\epsilon) & \beta_1 = 0, \gamma_2 > 0. \end{cases} \quad (58)$$

The proof is concluded by letting $\epsilon_0 \rightarrow 0^+$. □

All previous results are summarized in Table 1. To conclude this subsection, we make the following useful remark. {rem:gensip}

Remark 5. Let $a(\xi)$ be a continuous function for $\xi \in \mathbb{R}$ such that $\text{sgn}(a(\xi)) = -\text{sgn}(\xi)$ (hence $a(0) = 0$), and $0 < \sup_{\xi \in \mathbb{R}} |a(\xi)\xi^{-1}| \ll 1$. It is not hard to derive that the previously used SIP can be replaced by the more general SIP $\{z = \xi + a(\xi)\mathbf{i} : \xi \in \mathbb{R}\}$, as it ensures $\text{Im}(z^2) = 2\xi a(\xi) \ll \xi^2 - a^2(\xi) = \text{Re}(z^2)$, which all previous arguments only require.

3.3 Green's tensor in dissipative medium and limiting absorption principle

We are ready to justify the physical correctness of the prescribed Green tensor G by the limiting absorption principle. We shall overload $\mu_\pm^2(z^2)$, $\Delta(z^2)$, and $G(x; y)$ with $\mu_\pm^2(z^2; \rho\omega^2)$, $\Delta(z^2; \rho\omega^2)$, and $G^{\rho\omega^2}(x; y)$ respectively to emphasize their dependence on $\rho\omega^2$ in this subsection. Clearly,

$$\mu_\pm^2(z^2; \rho\omega^2) = \rho\omega^2 \mu_\pm^2(z^2/(\rho\omega^2); 1), \quad \Delta(z^2; \rho\omega^2) = \rho^2\omega^4 \Delta(z^2/(\rho\omega^2); 1). \quad (59) \quad \{\text{eq:rel}\}$$

For simplicity, we suppress the argument $\rho\omega^2$ if it equals 1 in the following. Now, let $\rho\omega^2 = 1 + \mathbf{i}\delta$ for $0 < \delta \ll 1$. Then, by (59) and by Remark 5, we may compute the related Green tensor $G^{1+\mathbf{i}\delta}$ based on the same idea in section 2 but directly use the real path, considering that $\{\xi(1 + \mathbf{i}\delta)^{-1/2} : \xi \in \mathbb{R}\}$ is a suitable SIP to well define $\sqrt{\mu_{\pm}^2(\xi^2/(1 + \mathbf{i}\delta))}$ and $\sqrt{\Delta(\xi^2/(1 + \mathbf{i}\delta))}$ according to Theorems 2, 3, and 4. Thus, we can define for $\xi \in \mathbb{R}$ that

$$\mu_{\pm}(\xi^2; 1 + \mathbf{i}\delta) := (1 + \mathbf{i}\delta)^{1/2} \sqrt{\mu_{\pm}^2(\xi^2/(1 + \mathbf{i}\delta))}, \quad (60) \quad \{\text{eq: def:1}\}$$

based on the prescribed branch cuts in Table 1. Nevertheless, it turns out that the branch cuts of $\sqrt{\mu_{\pm}^2(\xi^2; 1 + \mathbf{i}\delta)}$ are much simpler than $\sqrt{\mu_{\pm}^2(\xi^2/(1 + \mathbf{i}\delta))}$ due to the following lemma.

Lemma 4. *For any $\delta > 0$, the pathes $P_{\pm}^{\delta} := \{\mu_{\pm}^2(\xi^2; 1 + \mathbf{i}\delta) : \xi \in \mathbb{R}\}$ never touch the positive real axis. Thus, the following distance function*

$$\text{dist}(P_{\pm}^{\delta}, \mathbb{R}^+) \geq c(\delta), \quad \mathbb{R}^+ = [0, \infty), \quad (61) \quad \{\text{eq: dist}\}$$

for some strictly positive constant $c(\delta)$.

Proof. Observe (30). At most one of μ_{\pm}^2 touches the positive real axis at $\xi^2 = \xi_0^2 \geq 0$ and it must hold that

$$\Delta(\xi_0^2; 1 + \mathbf{i}\delta) = (a - \mathbf{i}\delta\beta_0)^2, \quad \beta_0 + \xi_0^2\beta_1 + a > 0. \quad (62) \quad \{\text{eq: tmp3}\}$$

for some constant a depending on ξ_0^2 . Compare the imaginary part to obtain $a = -(\alpha_0 + \alpha_1\xi_0^2)\beta_0^{-1}$, and then the real part to obtain that ξ_0^2 must be a root of

$$F(\eta) := (\alpha_2 - \alpha_1^2\beta_0^{-2})\eta^2 + 2\alpha_1\beta_0^{-2}(\beta_0^2 - \alpha_0)\eta + (\alpha_0\beta_0^{-2} + \delta^2)(\beta_0^2 - \alpha_0) = 0.$$

The inequality in (62) implies $0 < \xi_0^2 < 2(c_{11} + c_{33})^{-1}$. It is straightforward to verify from (C_0) that

$$\alpha_2 - \alpha_1^2\beta_0^{-2} < 0, \quad \beta_0^2 - \alpha_0 > 0,$$

Besides, it can be seen that $F(0) > 0$ and

$$F(2(c_{11} + c_{33})^{-1}) = \frac{4c_{22}c_{33}(c_{11} - c_{33})^2}{(c_{11} + c_{33})^2} + 4c_{22}c_{33}\delta^2 > 0,$$

implying $F(\xi_0^2) \geq 4c_{22}c_{33}\delta^2$ since F opens downward. The proof is finished by noticing that

$$|\text{Im}(\mu_{\pm}^2(\xi^2; 1 + \mathbf{i}\delta))| \geq \frac{(\beta_0 - \sqrt{\alpha_0})\delta}{4c_{33}c_{22}},$$

for $\xi^2 > C$, where $C > 0$ is a sufficiently large constant independent of δ . \square

Lemma 4 indicates that we can define $\mu_{\pm}(\xi^2; 1 + \mathbf{i}\delta)$ by directly choosing the positive real axis as the branch cut of $\sqrt{\mu_{\pm}^2(\xi^2; 1 + \mathbf{i}\delta)}$. This new definition coincides with (60) since both produce the same results at $\xi = \pm\infty$ and both are analytic for $\xi \in \mathbb{R}$. Due to the strictly positive distance of P_{\pm}^{δ} and \mathbb{R}^+ by (61), the real path can slightly move to $R_{\delta} := \{\xi + p(\delta)\mathbf{i} : \xi \in \mathbb{R}\}$ for some positive constant

$p(\delta) > 0$ so that $\mu_{\pm}^2((\xi + p(\delta)\mathbf{i})^2; 1 + \mathbf{i}\delta)$ are still strictly away from \mathbb{R}^+ and that $\min_{\xi \in \mathbb{R}} \text{Im}(\mu_{\pm}(\xi + p(\delta)\mathbf{i}; 1 + \mathbf{i}\delta)) \geq q(\delta)$ for some strictly positive constant $q(\delta)$. Consequently, by Cauchy's theorem, the real path used in (40-43) can be deformed to the new path R_{δ} . Since

$$\max_{z \in R_{\delta}} \text{Im}(\mu_{\pm}(z; 1 + \mathbf{i}\delta)|x_2| + z|x_1|) \geq p(\delta)|x_1| + q(\delta)|x_2|,$$

it is not hard to derive that for $|x| \gg 1$,

$$|G_{ij}^{1+\mathbf{i}\delta}(x)| \leq C(\delta)e^{-p(\delta)|x_1|/2 - q(\delta)|x_2|/2}, \quad i, j = 1, 2,$$

for some positive constant $C(\delta)$ independent of x . Therefore, $G^{1+\mathbf{i}\delta}(x)$ is dissipative in the sense that it decays exponentially at $|x| = \infty$. Moreover, by (59), (60) and by the change of variable $\xi/\sqrt{1 + \mathbf{i}\delta} \rightarrow \xi$, it is easy to deduce that

$$G^1(x) = \lim_{\delta \rightarrow 0^+} G^{1+\mathbf{i}\delta}(x), \quad |x| \neq 0.$$

Consequently, our proposed Green tensor for $\rho\omega^2 > 0$ singled out by the two fundamental principles (P1) and (P2) is the limit of dissipative Green's tensor, thus justifying its physical correctness.

3.4 Representative examples

To conclude this section, we list several representative examples below and shall study wave scattering problems in such media in sections 5 and 6. Note that we have excluded the trivial isotropic case.

(i). Media with $\min \Delta(\xi^2) \geq 0$:

$$(I) \quad c_{11} = 4, c_{22} = 20, c_{12} = 3.8, c_{33} = 2,$$

with $\gamma_2 \leq 0$;

$$(II) \quad c_{11} = 36, c_{22} = 1, c_{12} = 2, c_{33} = 1,$$

with $\gamma_2 > 0$.

(ii). Medium with $\min_{\xi \in \mathbb{R}} \Delta(\xi^2) \in (-\infty, 0)$:

$$(III) \quad c_{11} = 0.9, c_{22} = 10, c_{12} = 0.1, c_{33} = 1.$$

(iii). Media with $\min_{\xi \in \mathbb{R}} \Delta(\xi^2) = -\infty$:

$$(IV) \quad c_{11} = 0.9, c_{22} = 10, c_{12} = 2.5, c_{33} = 1, \quad (\beta_1 > 0)$$

$$(V) \quad c_{11} = 0.9, c_{22} = 10, c_{12} = \sqrt{10} - 1, c_{33} = 1, \quad (\beta_1 = 0)$$

$$(VI) \quad c_{11} = 0.9, c_{22} = 10, c_{12} = 2, c_{33} = 1, \quad (\beta_1 < 0)$$

with $\gamma_2 > 0$;

$$(VII) \quad c_{11} = 0.9, c_{22} = 10, c_{12} = 1.835, c_{33} = 1, \quad (\alpha_1 > 0, \alpha_2 < 0)$$

$$(VIII) \quad c_{11} = 0.9, c_{22} = 10, c_{12} = 1.5, c_{33} = 1, \quad (\alpha_1 < 0, \alpha_2 < 0)$$

$$(IX) \quad c_{11} = 0.9, c_{22} = 10, c_{12} = 1, c_{33} = 1, \quad (\alpha_2 = 0)$$

with $\gamma_2 \leq 0$.

Among them, we show the contours of $\mu_+^2(z^2)$ for media (II) and (VI) with $\gamma_2 > 0$, in Figure 1. Clearly, they cross the positive real axis, which cannot serve as their branch cuts.

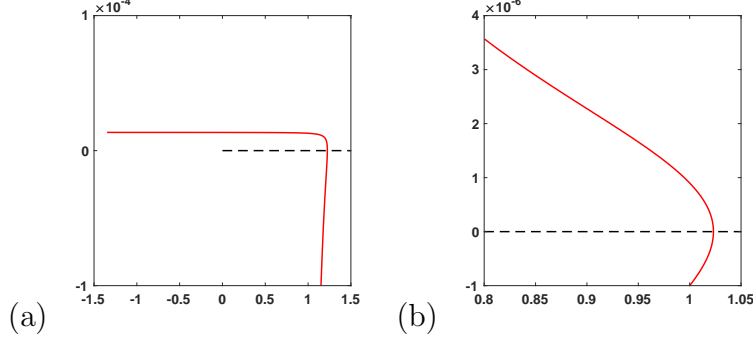


Figure 1: Contours of $\mu_+^2(z^2)$ for $\epsilon_0 = 10^{-5}$ around the positive real axis: (a) medium (II); (b) medium (VI). Dashed lines indicate the positive real axis. {fig:bc}

4 Fast evaluation of Green's tensor

In this section, we propose a fast algorithm for evaluating Green's tensor and its gradient. Without loss of generality, we assume $x_1, x_2 > 0$ and shall study $G_{11}(x)$ in detail only. Observe the coefficients $p_1^{x_1}$ and $q_1^{x_1}$ in (38) and (39). It can be seen that as $\xi^2 \rightarrow +\infty$,

$$p_1^{x_1}, q_1^{x_1} = \begin{cases} \mathcal{O}(|\xi|^{-1}), & \text{if } \alpha_2 \neq 0; \\ \mathcal{O}(1), & \text{if } \alpha_1 \neq 0, \alpha_2 = 0; \\ \mathcal{O}(|\xi|), & \text{if } \alpha_1 = 0, \alpha_2 = 0. \end{cases}$$

This suggests to study the three cases separately.

Case (i). Suppose $\alpha_2 = \alpha_1 = 0$. Then, it can be derived based on (C_0) that

$$0 < c_{12} + 2c_{33} = c_{11} = c_{22} > c_{33},$$

Let $c_{33} = \mu > 0$ and $c_{12} = \lambda$ so that $c_{11} = c_{22} = \lambda + 2\mu$ with $\lambda + \mu = c_{12} + c_{33} = c_{22} - c_{33} > 0$. Then, $\mu_+^2 = k_s^2 - \xi^2$ and $\mu_-^2 = k_p^2 - \xi^2$, where $k_s = \sqrt{\frac{1}{\mu}}$ and $k_p = \frac{1}{\sqrt{\lambda + 2\mu}}$. Thus,

$$p_1^{x_1} = \frac{\mathbf{i}\mu_+}{2}, \quad q_1^{x_1} = -\frac{\mathbf{i}\mu_-}{2} + \frac{k_p^2 \mathbf{i}}{2} \mu_-^{-1}, \quad p_2^{x_2} = -\frac{\mathbf{i}\xi}{2}.$$

By (4), we obtain

$$G_{11}(x) = k_s^2 \Phi_{k_s}(x) + \partial_{x_1}^2 (\Phi_{k_s}(x) - \Phi_{k_p}(x)). \quad (63)$$

One similarly obtains

$$G_{21}(x) = G_{12}(x) = \partial_{x_1 x_2}^2 (\Phi_{k_s}(x) - \Phi_{k_p}(x)), \quad (64)$$

$$G_{22}(x) = k_s^2 \Phi_{k_s}(x) + \partial_{x_2}^2 (\Phi_{k_s}(x) - \Phi_{k_p}(x)). \quad (65)$$

We have reproduced Green's tensor for an isotropic medium with Lamé constants λ and μ . As $|x| \rightarrow 0$, $\Phi_k(x) = -\frac{1}{2\pi} \log|x| + \mathcal{O}(|x|^2 \log|x|)$, it is easy to conclude that $G(x)$ exhibits logarithmic singularity as $|x| \rightarrow 0$. The evaluation of G and its gradient is straightforward.

Case (ii). Suppose now $\alpha_1 \neq 0$ and $\alpha_2 = 0$ so that $\beta_1 < 0$. To simplify the presentation, we consider $\alpha_1 > 0$ only. We find Taylor's expansions of $p_1^{x_1}$ and $q_1^{x_1}$ at $|\xi| = +\infty$,

$$p_1^{x_1}(\xi^2) e^{\mathbf{i}\mu_+(\xi^2)x_2} = e^{\mathbf{i}|\xi|p_0^+x_2} \sum_{n=0}^{\infty} \frac{c_n^+(x_2)}{|\xi|^n}, \quad (66) \quad \{\text{eq:exppx1}\}$$

$$q_1^{x_1}(\xi^2) e^{\mathbf{i}\mu_-(\xi^2)x_2} = e^{\mathbf{i}|\xi|p_0^-x_2} \sum_{n=0}^{\infty} \frac{c_n^-(x_2)}{|\xi|^n}, \quad (67) \quad \{\text{eq:expqx1}\}$$

where $p_0^\pm = p_0 = \lim_{\xi \rightarrow \infty} \mu_\pm(\xi^2)/|\xi| = \mathbf{i}\sqrt{4c_{11}/c_{22}}$,

$$c_0^+(x_2) = a_0 e^{\mathbf{i}b_0 x_2}, \quad c_0^-(x_2) = -a_0 e^{-\mathbf{i}b_0 x_2}, \\ a_0 = \lim_{\xi \rightarrow \infty} p_1^{x_1}(\xi^2), \quad b_0 = \lim_{\xi \rightarrow \infty} (\mu_+(\xi^2) - p_0|\xi|),$$

and the other coefficients $c_n^\pm(x_2)$ are smooth at $x_2 = 0$. Then, it can be seen that

$$G_{11}(x) = \frac{1}{2\pi} \int_{-M}^M \left[p_1^{x_1}(\xi^2) e^{\mathbf{i}\mu_+(\xi^2)x_2} + q_1^{x_1}(\xi^2) e^{\mathbf{i}\mu_-(\xi^2)x_2} \right] e^{\mathbf{i}\xi x_1} d\xi \\ + \frac{1}{2\pi} \sum_{n=0}^{\infty} \left[c_n^+(x_2) I_M^n(x; p_0^+) + c_n^-(x_2) I_M^n(x; p_0^-) \right], \quad (68) \quad \{\text{eq:G11:case2}\}$$

where $M > 0$ is a sufficiently large constant, and we have defined

$$I_M^n(x; \alpha) := \int_M^{+\infty} + \int_{-\infty}^{-M} \frac{e^{\mathbf{i}|\xi|\alpha x_2 + \mathbf{i}\xi x_1}}{|\xi|^n} d\xi, \quad \text{Im}(\alpha) > 0. \quad (69)$$

It can be seen that, for all $n \in \mathbb{N}$,

$$I_M^n(x; \alpha) = M^{1-n} [E_n(-M\mathbf{i}(\alpha x_2 + x_1)) + E_n(-M\mathbf{i}(\alpha x_2 - x_1))],$$

where $E_n(z) = z^{n-1} \int_z^{+\infty} t^{-n} e^{-t} dt$ is the generalized exponential integral (c.f. (8.19.2) in [29]). By (8.19.8) in [29],

$$E_0(z) = z^{-1} + \text{ANA}, \quad E_n(z) = -\frac{(-z)^{n-1}}{(n-1)!} \log z + \text{ANA}, \quad n \geq 1,$$

where ANA refers to some analytic function and the branch cut of \log is chosen as the negative real axis. Thus,

$$I_M^0(x; \alpha) = \frac{2\mathbf{i}\alpha x_2}{\alpha^2 x_2^2 - x_1^2} + \text{ANA}, \quad (70) \quad \{\text{eq:IM0}\}$$

$$I_M^n(x; \alpha) = \frac{-\mathbf{i}^{n-1}}{(n-1)!} \left[(\alpha x_2 + x_1)^{n-1} \log(\alpha x_2 + x_1) + (\alpha x_2 - x_1)^{n-1} \log(\alpha x_2 - x_1) \right] + \text{ANA}, \quad (71) \quad \{\text{eq:IMn}\}$$

so that, as $|x| \rightarrow 0^+$,

$$G_{11}(x) = \frac{2ip_0x_2a_0 \sin(b_0x_2)}{\pi(p_0^2x_2^2 - x_1^2)} - \frac{c_1^+(0) + c_1^-(0)}{2\pi} \log(-p_0^2x_2^2 + x_1^2) + o(1). \quad (72)$$

Considering that $p_0 = \mathbf{i}|p_0|$,

$$\left| \frac{2ip_0x_2a_0 \sin(b_0x_2)}{\pi(p_0^2x_2^2 - x_1^2)} \right| \leq \frac{2|a_0b_0|}{\pi|p_0|},$$

so that G_{11} exhibits logarithmic singularity at $z = 0$. In fact, it can be seen from (68), (70) and (71) that

$$G_{11}(x) = \frac{2ip_0x_2a_0 \sin(b_0x_2)}{\pi(p_0^2x_2^2 - x_1^2)} + \text{ANA} \times \log(p_0x_2 + x_1) + \text{ANA} \times \log(p_0x_2 - x_1) + \text{ANA}.$$

One similarly finds logarithmic singularities of $G_{12}(x)$ and $G_{22}(x)$ at $x = 0$.

To numerically evaluate G_{11} , we directly truncate the series in (68) at $n = N_0$. Empirically, N_0 and M are chosen such that $M^{-(N_0+1)} \leq \epsilon_T$, for some small error threshold $\epsilon_T > 0$. The functions $c_n^\pm(x_2)$, $n = 0, \dots, N_0$ can be precomputed via symbolic evaluation only once before the computation. The integral in (68) can be computed via the adaptive 16-point Gauss-Legendre quadrature rule. If we require G at a large amount of grid points of x , it becomes extremely costly to directly evaluate such an integral the same amount of times. To tackle this difficulty, we evaluate the integral at Chebyshev points of a sufficiently large rectangular domain enclosing the whole grid points, and then retrieve the targeted values by the simple Lagrange interpolation, considering that (68) is an analytic function of x .

To approximate the gradient of G_{11} , one directly differentiates (40) and then uses the same strategy as the above. The evaluation of G_{12} and G_{22} and their derivatives are similar; we omit the details.

Case (iii). Suppose now $\alpha_2 \neq 0$. The idea of computing G_{11} is still the same as that in Case (ii). But now c_0^+ and c_0^- in (66) and (67) are zero, and

$$p_0^\pm = \begin{cases} \sqrt{\frac{\beta_1 \pm \sqrt{\alpha_2}}{2c_{33}c_{22}}}, & \min_{\xi \in \mathbb{R}} \Delta(\xi^2) \notin (-\infty, 0), \\ \sqrt{\frac{\beta_1 \mp \sqrt{\alpha_2}}{2c_{33}c_{22}}}, & \min_{\xi \in \mathbb{R}} \Delta(\xi^2) \in (-\infty, 0). \end{cases}$$

Thus, it is easy to derive that, as $x \rightarrow 0$,

$$G_{11}^\pm(x) = c_1^\pm(0) \log((p_0^\pm)^2x_2^2 - x_1^2) + \mathcal{O}\left(\sqrt{(p_0^\pm)^2x_2^2 - x_1^2} \log((p_0^\pm)^2x_2^2 - x_1^2)\right) \quad (73) \quad \{\text{eq:G11:+-}\}$$

exhibiting the logarithmic singularity of G_{11} . The analysis of G_{12} and G_{22} is analogous to the previous case.

5 Exact TBC for any exterior scattering problem

In this section, we propose an exact TBC to truncate Navier's problem (18) in $\mathbb{R}^2 \setminus \overline{D}$. Let $B(O, r)$ be of sufficiently large radius $r > 0$ to enclose D . Let $\Omega = B(0, R) \setminus \overline{B(0, r)}$ for some constant $R > r$ and $\Gamma = \partial\Omega$ be its boundary. Using Green's tensor G , we obtain from the third Green's identity (c.f. Theorem 6.10 in [26]) that, for any $x \in \Omega$,

$$u(x) = \int_{\Gamma} [\mathcal{B}_{\nu(y)} G^T(y; x)]^T u(y) - G(y; x) \mathcal{B}_{\nu} u(y) ds(y),$$

where we recall that $\nu = [\nu_1, \nu_2]^T$ is the outer unit normal of the boundary Γ and \mathcal{B}_{ν} denotes the co-normal derivative operator given by

$$\mathcal{B}_{\nu} = [\mathcal{B}_{\nu}^{ij}]_{2 \times 2} := \nu_1 (A_{11} \partial_1 + A_{12} \partial_2) + \nu_2 (A_{21} \partial_1 + A_{22} \partial_2). \quad (74)$$

Inspired by SURC (7), we impose a new SURC for the scattered elastic wave u :

$$\lim_{R \rightarrow \infty} \int_{\partial B(0, R)} [\mathcal{B}_{\nu(y)} G^T(y; x)]^T u(y) - G(y; x) \mathcal{B}_{\nu} u(y) ds(y) = 0, \quad (75) \quad \{\text{eq:rc}\}$$

uniformly for x in any bounded domain. Its rigorous justification for $\rho\omega^2 > 0$ shall be presented in a future work elsewhere. For dissipative media with $\text{Im}(\rho\omega^2) > 0$, (75) is evident as the dissipative Green tensor G decays exponentially (c.f. section 3.3) and we must look for an exponentially decaying solution u .

This radiation condition directly leads to Green's exterior representation formula: for any $x \in \mathbb{R}^2 \setminus \overline{B(0, r)}$,

$$u(x) = \int_{\partial B(0, r)} [\mathcal{B}_{\nu(y)} G^T(y; x)]^T u(y) - G(y; x) \mathcal{B}_{\nu} u(y) ds(y). \quad (76) \quad \{\text{eq:grep}\}$$

By the standard jump relations (c.f. (7.5) in [26]), we obtain an exact TBC

$$(\mathcal{I}/2 - \mathcal{K})[u] = -\mathcal{S}[\mathcal{B}_{\nu} u], \quad \text{on } \partial B(0, r), \quad (77) \quad \{\text{eq:tbc}\}$$

where \mathcal{I} denotes the identity operator, the single- and double-layer potential operators \mathcal{S} and \mathcal{K} are defined by

$$\mathcal{S}[\phi] = \int_{\partial B(0, r)} G(y; x) \phi(y) ds(y), \quad (78)$$

$$\mathcal{K}[\phi] = p.v. \int_{\partial B(0, r)} [\mathcal{B}_{\nu(y)} G^T(y; x)]^T \phi(y) ds(y), \quad (79)$$

$\phi = [\phi_1, \phi_2]^T$, and $p.v.$ indicates Cauchy's principal value.

The TBC condition exactly truncates the unbounded scattering problem (18) onto the bounded domain $B(0, r) \setminus \overline{D}$ so that any standard solvers can apply readily. In this paper, we shall derive a BIE solver only for Navier's problem (18) based on the new TBC (77). To make the TBC applicable in practice, we require high-accuracy quadrature rules to discretize the integrals in (77).

5.1 High-accuracy discretization scheme

In this subsection, we propose a high-accuracy quadrature rule to discretize the two operators \mathcal{S} and \mathcal{K} . Consider the single-layer operator \mathcal{S} first. Let $\partial B(0, r)$ be parameterized by

$$x(t) = (x_1(t), x_2(t)) = (r \cos t, r \sin t), \quad 0 \leq t \leq 2\pi.$$

Thus,

$$\mathcal{S}[\phi](x(t)) = r \int_0^{2\pi} G(x(t) - x(\tilde{t})) \phi(x(\tilde{t})) d\tilde{t}. \quad (80) \quad \{\text{eq:dis:S}\}$$

Based on the discussion in section 4, it can be seen that the kernel tensor

$$G(x(t) - x(\tilde{t})) = \mathcal{O}(\log |t - \tilde{t}|), \quad \text{as } t - \tilde{t} \rightarrow 0.$$

Thus, we can simply use Alpert's six-order quadrature rule [1, 25] to discretize the integral in (80) based on a uniform discretization of t over $[0, 2\pi]$, i.e. $\{t_j = \frac{2j\pi}{N}\}_{j=0}^{N-1}$, to approximate

$$\mathcal{S}[\phi] \begin{bmatrix} x(t_0) \\ x(t_1) \\ \vdots \\ x(t_{N-1}) \end{bmatrix} \approx \begin{bmatrix} \mathbf{S}_{11} & \mathbf{S}_{12} \\ \mathbf{S}_{21} & \mathbf{S}_{22} \end{bmatrix} \begin{bmatrix} \phi_1 \\ \phi_2 \end{bmatrix},$$

where \mathbf{S}_{ij} denotes an $N \times N$ matrix and $\phi_j = [\phi_j(x(t_0)), \phi_j(x(t_1)), \dots, \phi_j(x(t_{N-1}))]^T$.

We now turn to the discretization of the double-layer operator \mathcal{K} given by

$$\mathcal{K}[\phi](x) = p.v. \int_{\partial B(0,r)} \begin{bmatrix} \mathcal{B}_{\nu(y)}^{11} G_{11} + \mathcal{B}_{\nu(y)}^{12} G_{21} & \mathcal{B}_{\nu(y)}^{21} G_{11} + \mathcal{B}_{\nu(y)}^{22} G_{21} \\ \mathcal{B}_{\nu(y)}^{11} G_{12} + \mathcal{B}_{\nu(y)}^{12} G_{22} & \mathcal{B}_{\nu(y)}^{21} G_{12} + \mathcal{B}_{\nu(y)}^{22} G_{22} \end{bmatrix} (x; y) \phi(y) ds(y). \quad (81) \quad \{\text{eq:BvG}\}$$

To simplify the presentation, we consider the case $\alpha_2 \neq 0$ only. Take

$$J(x) := \int_{\partial B(0,r)} \mathcal{B}_{\nu(y)}^{11} G_{11}(x; y) \phi_1 ds(y)$$

as an example. Based on the splitting of G , considering the logarithmic behavior of G_{11}^\pm in (73), we rewrite

$$\mathcal{B}_{\nu(y)}^{11} = f_1^\pm(y) [-(p_0^\pm)^2 \nu_1(y) \partial_1 + \nu_2(y) \partial_2] + f_2^\pm(y) \partial_\tau,$$

where τ denotes the unit tangential vector, and

$$f_1^\pm(y) = \frac{-c_{11}\nu_1^2(y) - c_{33}\nu_2^2(y)}{(p_0^\pm)^2 \nu_1(y)^2 - \nu_2(y)^2}, \quad f_2^\pm(y) = \frac{[(p_0^+)^2 c_{33} + c_{11}] \nu_1(y) \nu_2(y)}{(p_0^\pm)^2 \nu_1(y)^2 - \nu_2(y)^2}.$$

It can be verified that under (C_0) , $(p_0^\pm)^2$ are either negative or complex so that $(p_0^\pm)^2 \nu_1(y)^2 - \nu_2(y)^2 \neq 0$ for any $y \in \partial D$. Therefore, $f_j^\pm(x(t))$ are analytic for $t \in [0, 2\pi]$. Thus,

$$\mathcal{B}_{\nu(y)}^{11} G_{11}^\pm(x; y) = c_0^\pm(0) f_1(y) [-(p_0^\pm)^2 \nu_1(y) \partial_1 + \nu_2(y) \partial_2] \log((p_0^\pm)^2 (x_2 - y_2)^2 - (x_1 - y_1)^2)$$

$$+ \mathcal{B}_{\nu(y)}^{11}[G_{11}^{\pm}(x; y) - c_0^{\pm}(0) \log((p_0^{\pm})^2(x_2 - y_2)^2 - (x_1 - y_1)^2)] \\ + c_0^{\pm}(0) f_2^{\pm}(y) \partial_{\tau} \log((p_0^{\pm})^2(x_2 - y_2)^2 - (x_1 - y_1)^2).$$

As $x \rightarrow y$ along $\partial B(0, r)$, the sum of the first two terms is logarithmically singular by (73) and

$$\begin{aligned} & [- (p_0^{\pm})^2 \nu_1(y) \partial_1 + \nu_2(y) \partial_2] \log((p_0^{\pm})^2(x_2 - y_2)^2 - (x_1 - y_1)^2) \\ &= \frac{2(p_0^{\pm})^2 \nu_1(y)(y_1 - x_1) + 2\nu_2(y)(p_0^{\pm})^2(y_2 - x_2)}{(p_0^{\pm})^2(x_2 - y_2)^2 - (x_1 - y_1)^2} = \mathcal{O}(1). \end{aligned}$$

On the other hand,

$$\begin{aligned} & \int_{\partial B(0, r)} f_2(y) \partial_{\tau} \log((p_0^+)^2(x_2 - y_2)^2 - (x_1 - y_1)^2) \phi_1(y) ds(y) \\ &= - \int_{\partial B(0, r)} \log((p_0^+)^2(x_2 - y_2)^2 - (x_1 - y_1)^2) \frac{d}{ds} [f_2(y) \phi_1(y)] ds(y). \end{aligned}$$

Thus, the integrand of $J(x)$ is transformed into the sum of integrals of logarithmically singular integrands so that Alpert's quadrature applies to approximate

$$\mathbf{J} \approx \mathbf{A} \phi_1 + \mathbf{B}^+ \psi_1^+ + \mathbf{B}^- \psi_1^-,$$

for three $N \times N$ matrices \mathbf{A} and \mathbf{B}^{\pm} , where $\mathbf{J} = [J(x(t_0)), J(x(t_1)), \dots, J(x(t_{N-1}))]^T$, and

$$\begin{aligned} \psi_1^{\pm} &= \begin{bmatrix} \frac{d}{dt} [\phi_1(x(t)) f_2^{\pm}(x(t))] \big|_{t=t_0} \\ \frac{d}{dt} [\phi_1(x(t)) f_2^{\pm}(x(t))] \big|_{t=t_1} \\ \vdots \\ \frac{d}{dt} [\phi_1(x(t)) f_2^{\pm}(x(t))] \big|_{t=t_{N-1}} \end{bmatrix} = \mathbf{T}_1^{\pm} \phi_1 + \mathbf{T}_2^{\pm} \phi_1', \\ \mathbf{T}_1^{\pm} &= \text{Diag}\{[f_2^{\pm}]'(x(t_0)), \dots, [f_2^{\pm}]'(x(t_{N-1}))\}, \\ \mathbf{T}_2^{\pm} &= \text{Diag}\{f_2^{\pm}(x(t_0)), \dots, f_2^{\pm}(x(t_{N-1}))\}, \\ \phi_1' &= \text{Diag}\{\phi_1'(x(t_0)), \dots, \phi_1'(x(t_{N-1}))\}. \end{aligned}$$

Moreover, considering that $\phi(x(t))$ is a 2π -periodic smooth function for $t \in [0, 2\pi]$, we find, by the method of fast Fourier transform [37], a spectral-accuracy $N \times N$ differentiation matrix \mathbf{D} such that $\phi_1' = \mathbf{D} \phi_1$. Consequently,

$$\mathbf{J} \approx [\mathbf{A} + \mathbf{B}^+(\mathbf{T}_1^+ + \mathbf{T}_2^+ \mathbf{D}) + \mathbf{B}^-(\mathbf{T}_1^- + \mathbf{T}_2^- \mathbf{D})] \phi_1.$$

One similarly discretizes the other integrals in (81) to approximate

$$\mathcal{K}[\phi] \begin{bmatrix} x(t_0) \\ x(t_1) \\ \vdots \\ x(t_{N-1}) \end{bmatrix} \approx \begin{bmatrix} \mathbf{K}_{11} & \mathbf{K}_{12} \\ \mathbf{K}_{21} & \mathbf{K}_{22} \end{bmatrix} \begin{bmatrix} \phi_1 \\ \phi_2 \end{bmatrix}.$$

Then, the TBC (77) approximately becomes

$$\begin{bmatrix} \mathbf{I}/2 - \mathbf{K}_{11} & -\mathbf{K}_{12} \\ -\mathbf{K}_{21} & \mathbf{I}/2 - \mathbf{K}_{22} \end{bmatrix} \begin{bmatrix} \mathbf{u}_1 \\ \mathbf{u}_2 \end{bmatrix} \approx - \begin{bmatrix} \mathbf{S}_{11} & \mathbf{S}_{12} \\ \mathbf{S}_{21} & \mathbf{S}_{22} \end{bmatrix} \begin{bmatrix} \mathbf{v}_1 \\ \mathbf{v}_2 \end{bmatrix}, \quad (82) \quad \{\text{eq:app:tbc}\}$$

where $\mathbf{u}_j = [u_j(x(t_0)), \dots, u_j(x(t_{N-1}))]^T$ and $\mathbf{v}_j = [\mathcal{B}_{\nu} u_j(x(t_0)), \dots, \mathcal{B}_{\nu} u_j(x(t_{N-1}))]^T$.

The above discretization scheme for the smooth circle $\partial B(0, r)$ can be trivially extended to any smooth closed curves.

Medium	N	T_{prep}	T_{cal}	E_{inf}
(I)	80	14.2s	27.1s	1.5E-10
(II)	240	10.3s	228.9s	5.8E-10
(III)	100	12.3s	75.3s	2.1E-10
(IV)	200	11.7s	219.5s	3.5E-10
(V)	140	5.7s	134.9s	4.8E-10
(VI)	140	11.3s	101.7s	2.3E-10
(VII)	140	13.0s	97.0s	1.2E-10
(VIII)	100	11.7s	50.3s	3.5E-10
(IX)	100	14.5s	48.2s	3.4E-10

{tab:tbc}

Table 2: Accuracy of the proposed TBC for all media in section 3.3.

5.2 Numerical evidences

We now carry out numerical experiments to illustrate the correctness of the TBC (77). All numerical algorithms in this paper are implemented in MATLAB 2020a on a 2019 Macbook Pro.

Choose $r = 1$, $N_0 = 8$, $M = 20$, and let $u = G_1(x; x^*)$ be an elastic field excited by the source point $x^* = (0.3, 0) \in B(0, r)$. For all previous media in section 3.3 with $\rho = \omega = 1$, we choose proper values of N such that the following error quantity

$$E_{\text{inf}} = \left\| \begin{bmatrix} \mathbf{I}/2 - \mathbf{K}_{11} & -\mathbf{K}_{12} \\ -\mathbf{K}_{21} & \mathbf{I}/2 - \mathbf{K}_{22} \end{bmatrix} \begin{bmatrix} \mathbf{u}_1 \\ \mathbf{u}_2 \end{bmatrix} + \begin{bmatrix} \mathbf{S}_{11} & \mathbf{S}_{12} \\ \mathbf{S}_{21} & \mathbf{S}_{22} \end{bmatrix} \begin{bmatrix} \mathbf{v}_1 \\ \mathbf{v}_2 \end{bmatrix} \right\|_{\infty},$$

is less than 10^{-9} . The results are listed in Table 5.2. Here, T_{prep} records the running time for symbolically computing the coefficients $c_n^{\pm}(x_2)$ in (66) and (67) for G_{11} , and similar coefficients for the other components of G , and T_{cal} records the running time for evaluating E_{inf} . Results in Table 5.2 provide a solid evidence for the correctness of the TBC, regardless of the propagation behavior of wave fields at infinity. One may increase N to get more accurate approximations of the TBC. For example, we show the relation of E_{inf} against N for media (I), (III), (V) and (VIII) in Figure 2, where E_{inf} decays at a rate roughly proportional to N^{-6} , due to the order of accuracy of Alpert's rule we use.

If u and $\mathcal{B}_{\nu}u$ on $\partial B(0, r)$ are available, then, in the exterior domain $\mathbb{R}^2 \setminus \overline{B(0, r)}$, u can be computed via Green's representation formula (76). This is illustrated by Figure 3 for media (II), (IV), (VII) and (IX), where numerical and exact solutions for $G_{11}(x)$ are compared, and where dashed lines indicate the TBC boundary $\partial B(0, 1)$. Numerical solutions outside $B(0, 1)$ are obtained by using exact values of u and $\mathcal{B}_{\nu}u$ on $\partial B(0, 1)$. The indistinguishability of numerical and exact solutions provides another solid evidence for the correctness of the TBC (77).

6 Typical scattering problems

In this section, we consider two typical scattering problems to illustrate the effectiveness of the proposed TBC.

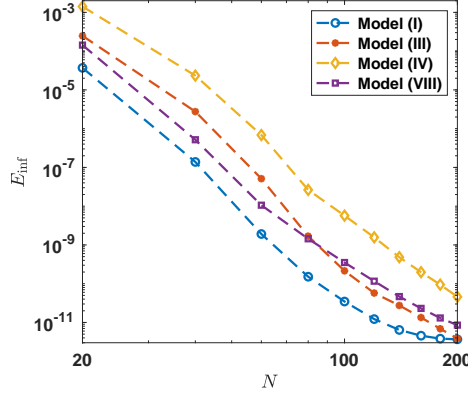


Figure 2: Error E_{inf} for the approximate TBC (82) against N for media (I), (III), (V) and (VIII).

{fig:err:N}

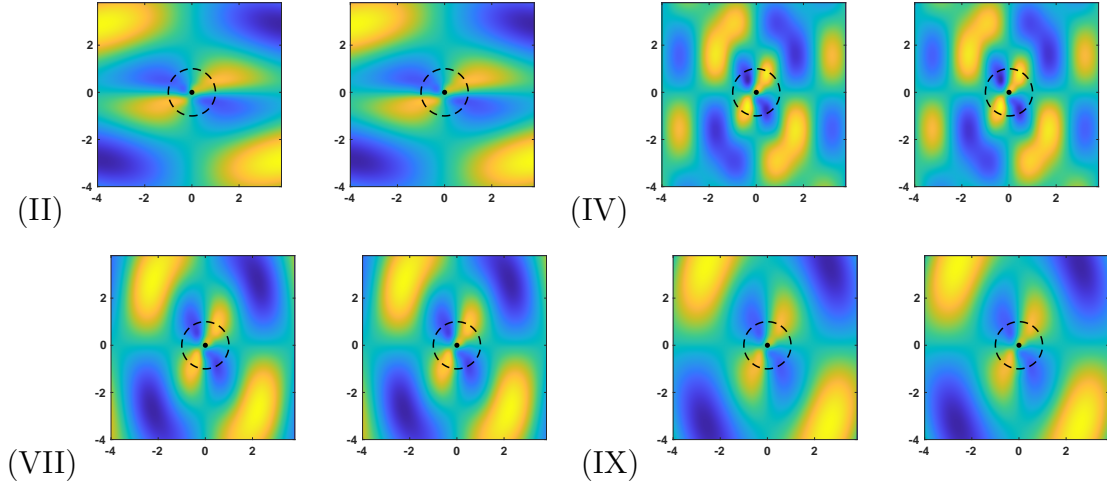


Figure 3: Comparisons of numerical solutions (right) and exact solutions (left) for $G_{11}(x)$ for media (II), (IV), (VII) and (IX) outside the TBC boundary $\partial B(0, 1)$ indicated by the dashed lines.

{fig:grerep}

6.1 Navier's Dirichlet-type problems

The Dirichlet problem in section 1.3 can now be completely posed as

$$-\partial_1(A_{11}\partial_1u + A_{12}\partial_2u) - \partial_2(A_{21}\partial_1u + A_{22}\partial_2u) - \rho\omega^2u = 0, \quad \text{in } \mathbb{R}^2 \setminus \overline{D}, \quad (83)$$

$$u|_{\partial D} = -u^{\text{inc}}|_{\partial D}, \quad (84) \quad \{\text{eq:p1bc}\}$$

$$u \text{ satisfies (75)}. \quad (85)$$

Here, the incident wave $u^{\text{inc}}(x)$ can be a point-source wave $G_j(x; x^*)$, $j = 1, 2$, excited by a specified source point $x^* \notin \overline{D}$ or a plane wave $u^0 e^{i\sqrt{\rho}\omega x \cdot d}$, with a nonzero polarization vector $u^0 = [u_1^0, u_2^0]^T$ and a directional vector $d = [d_1, d_2]^T$, determined in advance by

$$\begin{bmatrix} c_{11}d_1^2 + c_{33}d_2^2 & (c_{12} + c_{33})d_1d_2 \\ (c_{12} + c_{33})d_1d_2 & c_{33}d_1^2 + c_{22}d_2^2 \end{bmatrix} u^0 = u^0. \quad (86) \quad \{\text{eq:plane:inc}\}$$

To solve this unbounded domain problem, we directly make use of the TBC (77) on ∂D . Then,

$$\mathcal{B}_\nu u = \mathcal{S}^{-1}(\mathcal{I}/2 - \mathcal{K})[u^{\text{inc}}], \quad \text{on } \partial D. \quad (87) \quad \{\text{eq:method1}\}$$

Based on the high-accuracy discretization scheme in section 5.1, $\mathcal{B}_\nu u$ can be accurately approximated. Once $\mathcal{B}_\nu u$ on ∂D becomes available, Green's exterior representation formula (76) applies to get u in $\mathbb{R}^2 \setminus \overline{D}$. One might argue for an indirect approach to formulate the problem into a second-kind Fredholm equation, but this is not the aim of the current paper.

6.2 Navier's Neumann-type problems

A Neumann problem replaces (84) with

$$\mathcal{B}_\nu u|_{\partial D} = -\mathcal{B}_\nu u^{\text{inc}}|_{\partial D}. \quad (88) \quad \{\text{eq:p2bc}\}$$

It models wave scattered by an artificial elastic obstacle D with the property

$$\mathcal{B}_\nu u^{\text{tot}} = \mathcal{B}_\nu u + \mathcal{B}_\nu u^{\text{inc}} = 0, \quad \text{on } \partial D,$$

where we recall u^{tot} denotes the total wave field $u + u^{\text{inc}}$. Now, the TBC (77) implies

$$u = (\mathcal{I} - \mathcal{K})^{-1} \mathcal{S}[\mathcal{B}_\nu u^{\text{inc}}],$$

and then Green's exterior representation formula (76) applies to get u in $\mathbb{R}^2 \setminus \overline{D}$.

6.3 Numerical experiments

We study three specific examples to illustrate the accuracy of the proposed approach.

Let D be a kite-shaped domain with boundary ∂D parameterized by

$$x(t) = (\cos(2\pi t) + 0.65 \cos(4\pi t) - 0.65, 1.5 \sin(2\pi t)), \quad 0 \leq t \leq 1. \quad (89) \quad \{\text{eq:kite}\}$$

We consider two incident waves: (1) a plane wave $u_{\text{pw}}^{\text{inc}}(x) = A_0 e^{i\sqrt{\rho}\omega x \cdot d}$ with a normalized vector A_0 and $d = d_2[\sqrt{\frac{c_{33}}{c_{11}}}, 1]^T$ satisfying (86); (2) a point-source wave $u_{\text{ps}}^{\text{inc}}(x) = G_1(x; x^*)$ with $x^* = (0, 3) \notin D$.

In the implementation, we assume $\rho = \omega = 1$, let $M = 20$ in (68) and then truncate the series after $n = 8$ to evaluate G_{11} and, similarly, the other components in G as well as their derivatives. Define

$$\text{Relative error} = \frac{\|\phi_{\text{num}} - \phi_{\text{ref}}\|_{\text{inf}}}{\|\phi_{\text{ref}}\|_{\infty}},$$

where ϕ_{num} represents a numerical solution of the co-normal derivative $\mathcal{B}_\nu u$ for Dirichlet problems or that of the scattered field u for Neumann problems, at the N grid points on ∂D , and ϕ_{ref} represents a reference solution, obtained for a sufficiently large number N .

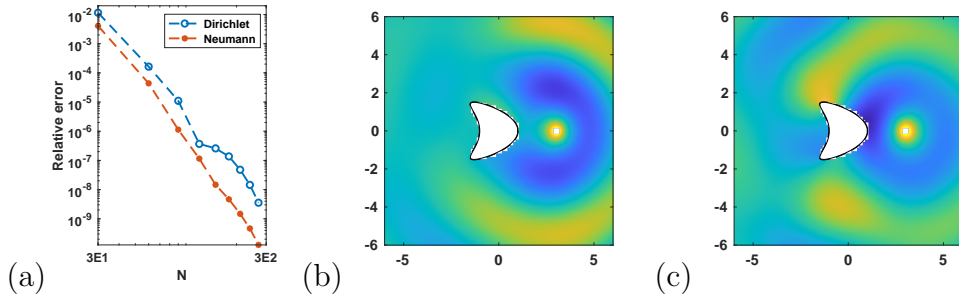


Figure 4: Scattering problems for medium (III) with the point-source incidence u_{ps}^{inc} : (a) relative error vs. N ; (b) real part of u_1 for the Dirichlet problem; (c) real part of u_1 for the Neumann problem. {fig:M3:ps}

First, we study the Dirichlet and Neumann problems for medium (III) by specifying the point-source incident wave u_{ps}^{inc} . Numerical results are shown in Figure 4, where (a) shows relative error against N with both axes in logarithmic scale, and (b) and (c) show real parts of u_1 in $[-6, 6]^2$ for Dirichlet and Neumann problems, respectively.

Second, we study the Dirichlet and Neumann problems for medium (VI) by specifying the plane incident wave u_{pw}^{inc} . Numerical results are shown in Figure 5, where (a) shows relative error against N , and (b) and (c) show real parts of u_1 in

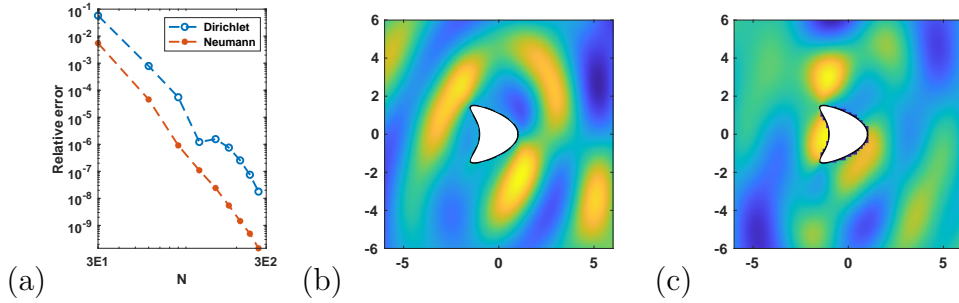


Figure 5: Scattering problems for medium (VI) with the plane-wave incidence u_{pw}^{inc} : (a) relative error vs. N ; (b) real part of u_1 for the Dirichlet problem; (c) real part of u_1 for the Neumann problem. {fig:M7:pw}

$[-6, 6]^2$ for Dirichlet and Neumann problems, respectively.

To conclude this section, in the last example, suppose D consists of two well separated domains: the previously introduced kite-shaped domain (89) centered at $(3, 3)$ and a disk of radius 2 centered at $(-3, -3)$. Clearly, it loses efficiency to use a big circle to enclose D , as it enlarges the computational domain. Alternatively, we can directly establish the TBC (77) on ∂D . We study the Neumann problem for medium (IV) for both the point-source incidence u_{ps}^{inc} and the plane-wave incidence u_{pw}^{inc} . The results are shown in Figure 6, where (a) shows relative error against N , and (b) and (c) show real parts of u_1 in $[-8, 8]^2$ for the point-source incidence u_{ps}^{inc} and the plane-wave incidence u_{pw}^{inc} , respectively.

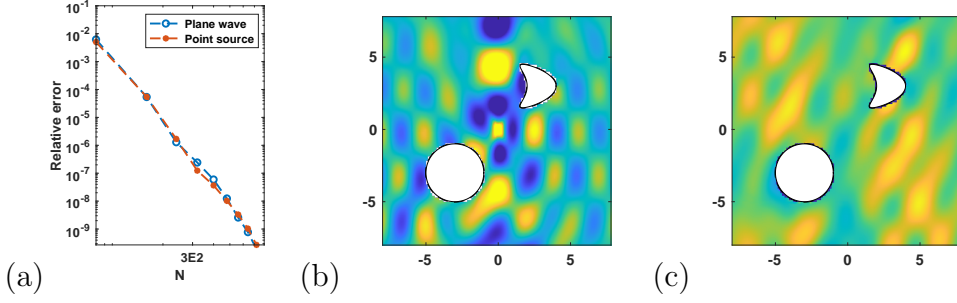


Figure 6: Neumann scattering problems for medium (IV): (a) relative error vs. N ; (b) real part of u_1 for the point-source incidence $u_{\text{ps}}^{\text{inc}}$; (c) real part of u_1 for the plane-wave incidence $u_{\text{pw}}^{\text{inc}}$.

{fig:M4:neu}

7 Conclusions and Discussions

We derived two-dimensional elastodynamic Green's tensor in anisotropic media by the method of Fourier transform and the use of SIP, and presented a rigorous theory to completely classify the propagation behavior of Green's tensor for any tensor C satisfying (C_0) . Based on Green's tensor, we introduced a new SURC (75) to characterize elastic scattered waves at infinity due to bounded scatterers. Based on (75), the simple TBC (77) in terms of single- and double-layer integral operators were used to analytically truncate the scattered waves, whether backward waves exist or not. A number of numerical experiments have validated the correctness of the TBC. Nevertheless, many significant problems arise and deserve to be studied. We list a few but certainly incomplete problems below.

Firstly, an essential problem is: how to rigorously justify the correctness of the new SURC (75)? We believe that this can be solved by directly proving the well-posedness of the scattering problem in $H_{\text{loc}}^1(\mathbb{R}^2 \setminus \overline{D})$ under (75).

The second problem is: how to simplify the new SURC (75)? Based on the relation of SRC (3) with SURC (7), we believe that this problem can be solved by carefully analyzing the asymptotic behavior of $G(x)$ for $|x| \gg 1$.

Considering that the exact TBC (77) is a nonlocal boundary condition, the third problem is: whether a PML-like local boundary condition exists or not? Discouragingly, the answer might be “No”, as it is impossible to transform waves such as $c_1 e^{ik_1 x_2} + c_2 e^{-ik_2 x_2}$, $k_j > 0$, to exponentially decaying waves due to the completely different behavior at their essential singularities in \mathbb{C} .

The fourth problem is: how to extend the current approach to more general media, e.g., general anisotropic media with $c_{13}c_{23} \neq 0$, three-dimensional general anisotropic media, etc.? Based on the same idea, the results must be as simple as these stated in Theorems 2, 3, and 4 of the current paper, although the derivations are tolerably tedious.

The last, most significant problem is: how to extend the current approach to time-domain problems? An immediate approach might be Fourier inverse transforming frequency-domain Green's tensor to get time-domain Green's tensor so as to derive a time-domain TBC.

References

- [1] B. K. Alpert. Hybrid Gauss-trapezoidal quadrature rules. *SIAM Journal on Scientific Computing*, 20(5):1551–1584, 1999.
- [2] H. Ammari, G. Bao, and A. W. Wood. An integral equation method for the electromagnetic scattering from cavities. *Math. Methods Appl. Sci.*, 23:1057–1072, 2000.
- [3] D. Appelö and G. Kreiss. A new absorbing layer for elastic waves. *J. Comput. Phys.*, 215:642–660, 2006.
- [4] G. Bao, L. Xu, and T. Yin. An accurate boundary element method for the exterior elastic scattering problem in two dimensions. *J. Comput. Phys.*, 348(1):343–363, 2017.
- [5] E. Bécache, A.-S. Bonnet-Ben Dhia, S. Fliss, and A. Tonnior. The half-space matching method for elastodynamic scattering problems in unbounded domains. *hal-03793031*, 2022.
- [6] E. Bécache, S. Fauqueux, and P. Joly. Stability of perfectly matched layers, group velocities and anisotropic waves. *J. Comput. Phys.*, 188:399–433, 2003.
- [7] J.-P. Berenger. A perfectly matched layer for the absorption of electromagnetic waves. *J. Comput. Phys.*, 114(2):185 – 200, 1994.
- [8] J. M. Carcione. *Wave fields in real media: Wave propagation in anisotropic, anelastic, porous and electromagnetic media (Third Edition)*. Elsevier, 2015.
- [9] Z. Chen and H. Wu. An adaptive finite element method with perfectly matched absorbing layers for the wave scattering by periodic structures. *SIAM J. Numer. Anal.*, 41(3):799–826, 2003.
- [10] Z. Chen, X. Xiang, and X. Zhang. Convergence of the pml method for elastic wave scattering problems. *Math. Comp.*, 85:2687–2714, 2016.
- [11] Z. Chen and W. Zheng. Convergence of the uniaxial perfectly matched layer method for time-harmonic scattering problems in two-layered media. *SIAM J. Numer. Anal.*, 48:2158–2185, 2010.
- [12] Z. Chen and W. Zheng. Pml method for electromagnetic scattering problem in a two-layer medium. *SIAM J. Numer. Anal.*, 55:2050–2084, 2017.
- [13] W. C. Chew and W. H. Weedon. A 3D perfectly matched medium for modified Maxwell’s equations with stretched coordinates. *Microwave and Optical Technology Letters*, 7(13):599–604, 1994.
- [14] D. Colton and R. Kress. *Inverse Acoustic and Electromagnetic Scattering Theory (3rd Edition)*. Springer, 2013.

- [15] B. Engquist and A. Majda. Absorbing boundary conditions for the numerical simulation of waves. *Math. Comp.*, 31(139):629–651, 1977.
- [16] Y. Gao and W. Lu. Wave scattering in layered orthotropic media i: a stable PML and a high-accuracy boundary integral equation method. *SIAM J. Sci. Comput.*, 44(4):B861–B884, 2022.
- [17] K. Gerdes and L. Demkowicz. Solution of 3d-laplace and helmholtz equations in exterior domains using hp-infinite elements. *Comput. Methods Appl. Mech. Engrg.*, 137:239–273, 1996.
- [18] J. Joannopoulos, S. G. Johnson, J. Winn, and R. Meade. *Photonic Crystals: Molding the flow of light (Second Edition)*. Princeton University Press, 2008.
- [19] R. Kress. *Linear Integral Equations (3rd Edition)*. Springer, 2014.
- [20] V. D. Kupradze, T. G. Gegelia, M. O. Basheleishvili, and T.V. Burchuladze. *Three-Dimensional Problems of the Mathematical Theory of Elasticity and Thermoelasticity*. North-Holland, Amsterdam, 1979.
- [21] M. Lassas and E. Somersalo. Analysis of the PML equations in general convex geometry. *Proceedings of the Royal Society of Edinburgh: Section A Mathematics*, 131(5):1183–1207, 2001.
- [22] G. R. Liu and K. Y. Lam. Two-dimensional time-harmonci elastodynamic green’s functions for anisotropic media. *Int. J. Engng Sci.*, 34(11):1327–1338, 1996.
- [23] W. Lu. Mathematical analysis of wave radiation by a step-like surface. *SIAM J. Appl. Math.*, 81(2):666–693, 2021.
- [24] W. Lu, J. Lai, and H. Wu. On wellposedness and convergence of upml method for analyzing wave scattering in layered media. *arXiv preprint arXiv:1910.13932*, 2019.
- [25] W. Lu, Y. Y. Lu, and J. Qian. Perfectly matched layer boundary integral equation method for wave scattering in a layered medium. *SIAM J. Appl. Math.*, 78(1):246–265, 2018.
- [26] W. McLean. *Strongly Elliptic Systems and Boundary Integral Equations*. Cambridge University Press, New York, NY, 2000.
- [27] P. Monk. *Finite Element Methods for Maxwell’s Equations*. Oxford University Press, 2003.
- [28] C. Muller. *Grundprobleme de mathematischen Theorie elektromagnetischer Schwingungen*. Berlin: Springer, 1957.
- [29] F. W. Olver, D. W. Lozier, R. F. Boisvert, and C. W. Clark. *NIST Handbook of Mathematical Functions*. Cambridge University Press, New York, NY, 2010.

- [30] J. A. Roden and S. D. Gedney. Convolution pml (cpml): An efficient fdtd implementation of the cfs-pml for arbitrary media. *Microwave and Optical Technology Letters*, 27:334–339, 2000.
- [31] S. Savadatti and M. N. Guddati. Accurate absorbing boundary conditions for anisotropic elastic media. part 1: Elliptic anisotropy. *J. Comput. Phys.*, 231:7584–7607, 2012.
- [32] S. Savadatti and M. N. Guddati. Accurate absorbing boundary conditions for anisotropic elastic media. part 2: Untilted non-elliptic anisotropy. *J. Comput. Phys.*, 231:7608–7625, 2012.
- [33] S. H. Schot. Eighty years of Sommerfeld’s radiation condition. *Historia Mathematica*, pages 385–401, 1992.
- [34] S. Silver. *Microwave antenna theory and design*. (M.I.T. Radiation Laboratory Series. No. 12.) New York: McGraw-Hill, 1949.
- [35] A. Sommerfeld. Die Greensche Funktion der Schwingungsgleichung. *Jahresbericht der Deutschen Mathematiker-Vereinigung*, 21:309–353, 1912. Reprinted in *Gesammelte Schriften*, Vol. 1, pp. 272-316.
- [36] A. Taflov and S. C. Hagness. *Computational Electrodynamics: The Finite Difference Time Domain Method, Third Edition*. Artech House, Boston, London, 2005.
- [37] L. N. Trefethen. *Spectral Methods in MATLAB*. SIAM, 2000.
- [38] X. Yu, G. Hu, W. Lu, and A. Rathsfeld. PML and high-accuracy boundary integral equation solver for wave scattering by a locally defected periodic surface. *SIAM J. Numer. Anal.*, 60(5):2592–2625, 2022.